論文 / 著書情報
Article / Book Information

論題(和文)	
Title	Archaeology with GIS in the Indus Project
著者(和文)	寺村裕史, 近藤康久, 宇野隆夫
Authors	Hirofumi Teramura, Yasuhisa Kondo, Takao Uno
出典 / Citation	, , , pp. 165-196
Citation(English)	Excavation at Kanmer: 2005-06 – 2008-09. Kanmer Archaeological Research Project an Indo-Japanese Collaboration, , , pp. 165-196
発行日 / Pub. date	2012, 3

Author's copy

CHAPTER 5
GIS AND ELECTROMAGNETIC SURVEY

EXCAVATION AT KANMER: 2005-06 – 2008-09

KANMER ARCHAEOLOGICAL RESEARCH PROJECT AN INDO- JAPANESE COLLABORATION

Editor: J. S. Kharakwal, Y. S. Rawat and Toshiki Osada

ISBN: 978-4-902325-72-0

Indus Project, Research Institute for Humanity and Nature (RIHN)

457-4 Motoyama, Kamigamo, Kita-ku, Kyoto 603-8047 Japan

Tel: +81-75-707-2371 Fax: +81-75-707-2508

E-mail: osada@chikyu.ac.jp

Printed in Kyoto, Japan by Nakanishi Printing Co. Ltd.

CHAPTER 5

GIS AND ELECTROMAGNETIC SURVEY

1. Archaeology with GIS at Kanmer

Hirofumi Teramura, Yasuhisa Kondo, Takao Uno

Introduction

The Harappan Civilization is known as one of the early civilizations in the world. It flourished in the vast areas covering Pakistan and the northwest part of India during the third millennium BCE, mainly divided into three chronological phases: the Early, Mature and Late Harappan periods.

The civilization is characterized by well-planned quadrate urban settlements in various size, well-designed pottery, precious stone, shell, faience or metal ornaments as a fruit of the highly sophisticated production technology, and copper/stone seals with scripts and human/animal representations (Wheeler 1968, Kenoyer 1998, Possehl 1999, Agrawal and Kharakwal 2003, Osada 2005).

On the other hand, archaeological studies have revealed that there is no evidence of the powerful political leaders suggested by palace or royal tomb and also very few traces indicating the development of weapons in this civilization (Ibid.). Nevertheless it prospered with sustainable agriculture and animal husbandry in the Greater Indus Plain through which the Indus and Ghaggar-Hakra rivers used to run, as well as active interactions with the Iranian, Gulf and Mesopotamian civilizations to the west, BMAC (Bactria-Margiana Archaeological Complex) in Afghanistan and the adjacent regions to the north, the Neolithic communities in the Ganges Valley to the east and those in South India to the south (Ibid.).

However, many aspects of the Harappan culture still remain to be clarified due to an inadequate number of archaeological excavations by means of multidisciplinary and scientific approaches. Firstly, for instance, the formation process of the Harappan subsistence economy should be understood in more detail because its fauna and flora consisted of not only domestic animals (sheep and goat) and plants (wheat, barley and peas) originated in southwest Asia but also those from other regions (rice, zebu and horse). Secondly, the rise and fall of the Harappan Civilization, which has been long debated and often explained by either the environmental change or the immigration (Ibid., see also Osada 2001), should scientifically be examined.

Considering this situation, the Project "Environmental Change and the Indus Civilization" (the Indus Project) has been organized by Professor Toshiki Osada and Research Institute of Humanities and Nature, Kyoto in order to understand the formation, development and decline of the Harappan Civilization and the impact of the environmental change on those by means of an interdisciplinary approach. A number of researchers from different academic backgrounds − archaeology, geology, linguistics and anthropology for example − are working in collaboration, belonging to one of the four research groups: material culture, paleoenvironment, inherited culture and subsistence system.

Integrating and publishing results provided by different research groups as a coherent achievement is a big issue of such a multidisciplinary project. In order to accomplish this task, the authors, archaeology-GIS team in the material culture research group, have been employing GIS (Geographic Information Systems) as a common platform to share, manage and analyze all the study resources in an integrated fashion, by attaching temporal-spatial information.

Our team has been developing the methodological framework for general survey and excavation of the Harappan sites, according to the above-mentioned objectives of the Indus Project. In our scheme, all the data obtained in the field are managed by GIS. Those data are tagged with the geodetic coordinate (latitude and longitude or UTM coordinate based on WGS84; World Geodetic System 1984) determined by high-precision GPS (Global Positioning System), Total Station or photogrammetric instruments. The authors have also been assembling a large database of the Harappan settlements to analyze their distribution as well as conducting digital topographic survey of the selected sites and photogrammetry of the built remains in the field campaign.

This chapter reports the results of this approach - archaeology with GIS in the Indus Project. The main objective of the research is to digitally document archaeological remains as accurately as possible. This will enable us to manage archaeological finds from different sites in a unified format to compare at the same scale and with the same criteria. The authors also intend this study for a basic model of archaeological investigations in the Digital Era. Through this project, we would like to publish the archaeological data that are relevant to comparative studies with an interdisciplinary approach.

1. Process of Research

The Indus Project has been putting GIS-aided archaeology into practice since the planning phase. This paragraph overviews the process of GIS-based research in this project (Figure 5.1.1).

First of all, as a pilot study, Hirofumi Teramura prepared the Digital Elevation Model (DEM) covering Pakistan and the northwest part of India as well as the database including more than 2,000 sites which are associated with the Harappan Culture (from the Neolithic to the Early Iron Age; see also section 7 in this article), clearly dated and georeferenced, in between April 2005 and March 2006. Based on these data and by means of the analytical modules installed in the GIS software packages (IDRISI and ArcGIS), a series of time-sliced distribution maps of the archaeological sites were created and also a number of spatial analyses, such as site distribution density evaluation, run-off reconstruction and sea level change simulation, were carried out. The results of these analyses were served for assessing the diachronic change of the distribution of the Harappan-related sites and the spatial relationship between the settlements and the drainages.

In February 2006, in parallel with the first excavation at the Harappan site of Kanmer, Takao Uno conducted a topographic survey of the citadel and its periphery. The ground surface was surveyed on foot, with an antenna pole carried on the back and connected with a GPS receiver (Trimble Pro XH) as mobile station to determine the walker's position once in a second. The GPS data were calibrated by Kengo Miyahara (Kyoto City Archaeological Research Institute). The calibrated data were served for creating a DEM of the citadel and its periphery (by Teramura). It has been utilized as a base map since then to display the data acquired from the excavations as well as

Figure 5.1.1 Major archaeological sites mentioned in the text

used for the analysis of visibility from the citadel.

In February 2007, in parallel with the second season of the excavations at Kanmer, Hirofumi Teramura, Yasuhisa Kondo and Takao Uno conducted a photogrammetric survey of the uncovered architecture. The topography of the stone walls of the citadel was also surveyed with the aid of differential GPS receivers (Topcon GB500 and GB1000) operated by Kengo Miyahara.

In the next month, Takao Uno surveyed the Harappan sites in the Ghaggar and Chautang Valleys in the states of Haryana and Rajastan, India, together with Professor Vasant Shinde and his colleagues. In the survey, by means of GPS, the sites were profiled and some ground control points were allocated for the future excavations (see also Osada and Uesugi eds. 2008).

In February 2008, Hirofumi Teramura, Yasuhisa Kondo and Takao Uno, in collaboration with Hajime Chiba (Tohoku Gakuin University), carried out a topographic survey at Farmana, one of the Harappan sites that surveyed in Haryana in the previous season to be selected for excavation. Teramura and Kondo integrated the results of the profiling and the topographic survey into a DEM of the site (section 3). In that season, the third campaign at Kanmer was also supported by the GIS team to conduct the topographic survey using a Total Station with prism-based automatic tracking facility (Trimble S6) in order to provide a new DEM.

In addition, Uno surveyed the topography of Kanmer East, another site discovered on the hill located to the east of the citadel by means of a couple of differential GPS receivers (Topcon GB1000). Furthermore, a Ground Penetrating Radar (GPR) survey of the Kanmer citadel was conducted by Hideo Sakai, Toru Kishida and Asuka Kanto. A photogrammetric survey of the

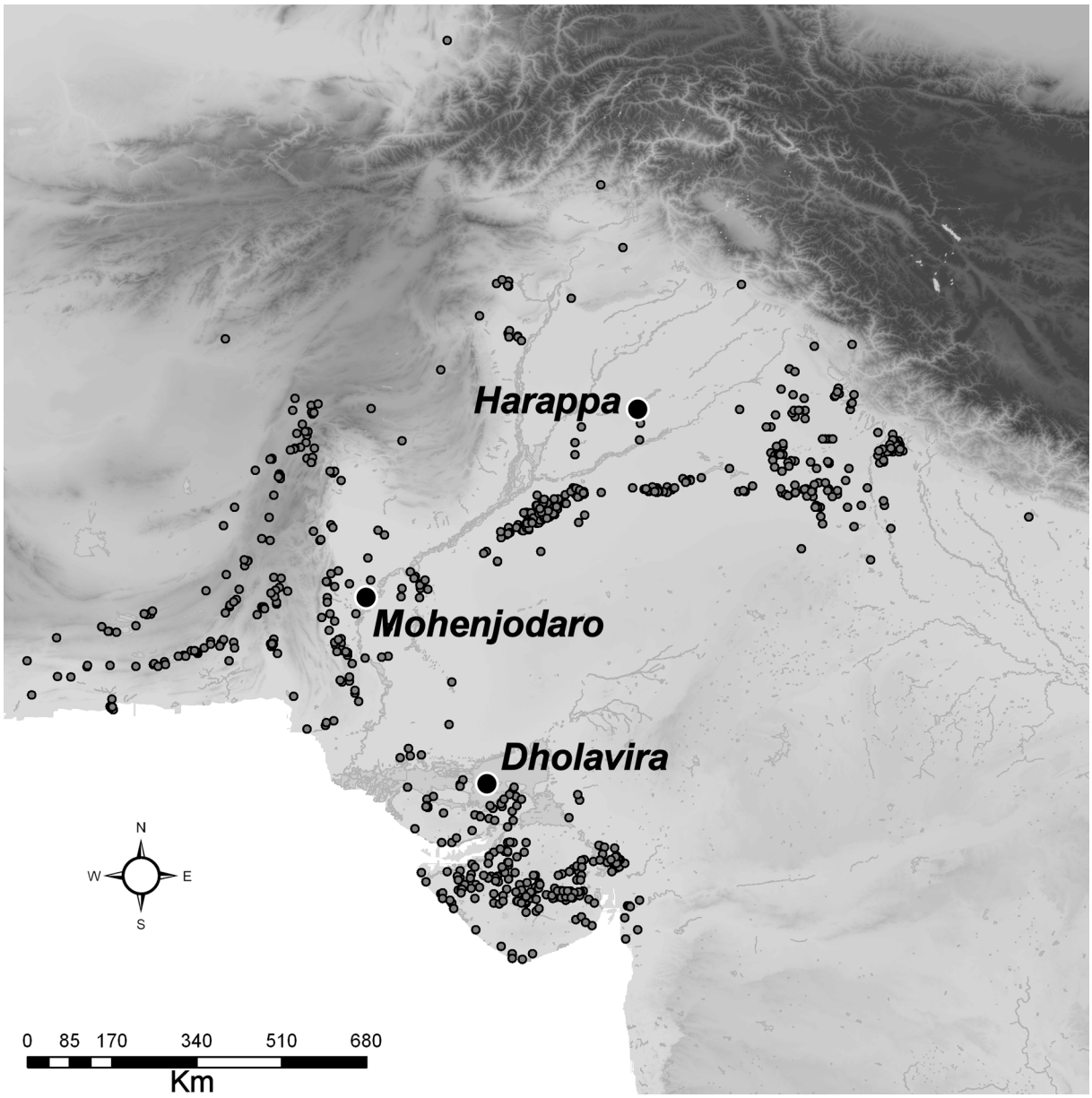

Figure 5.1.2 Distribution of the Mature Harappan sites

Figure 5.1.3 Archaeology-GIS team working with a GPS receiver (left) and Total Station (right)

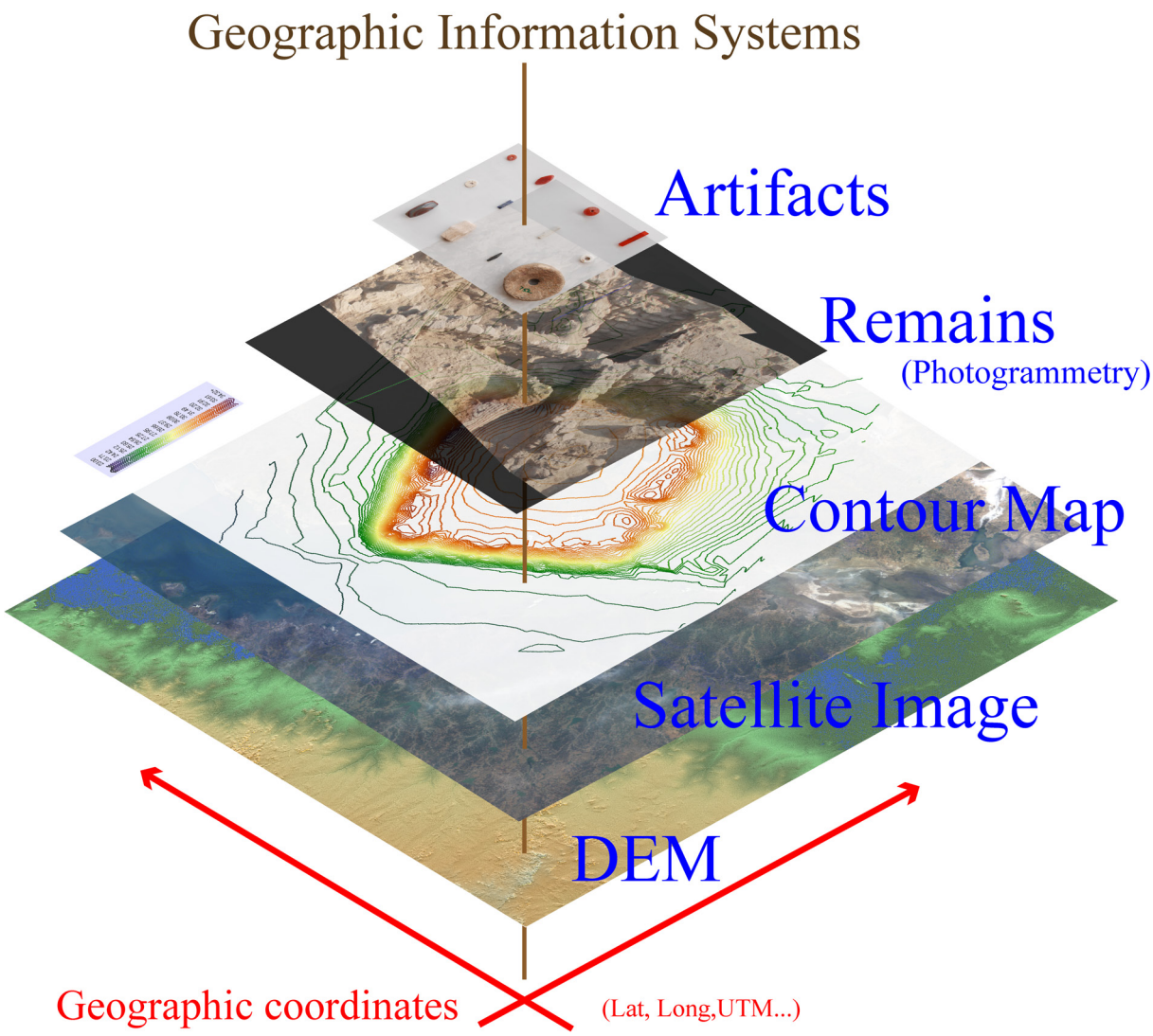

Figure 5.1.4 Scheme of integration geo-spatial datasets by GIS in the Indus Project

unearthed architectural remains was also carried out.

2. Methodology

As mentioned in the introductory part, the Indus Project aims at understanding the impact of the paleoenvironment on the Harappan Civilization in terms of the human adaptation to the environment through time. The task of the archaeology-GIS team in the project is to integrate various data obtained from the excavations in GIS to collect, manage, analyze and publish the information in a unified manner.

The actual research has been designed and conducted at three analytical scales: (1) supra-regional, (2) regional and (3) target site levels. First, the supra-regional level analyses include the database building for the Harappan sites and the assessment of the site distribution with the analytical tools packaged in GIS and that database (Figure 5.1.2; see also section 7 in this article). The diachronic change of the distribution and density of settlements are analyzed from the wider view point covering India and Pakistan. Second, at the regional level, the relationship between the site location and the environment is analyzed by the drainage reconstruction in Haryana and the simulation of sea level change and visibility in

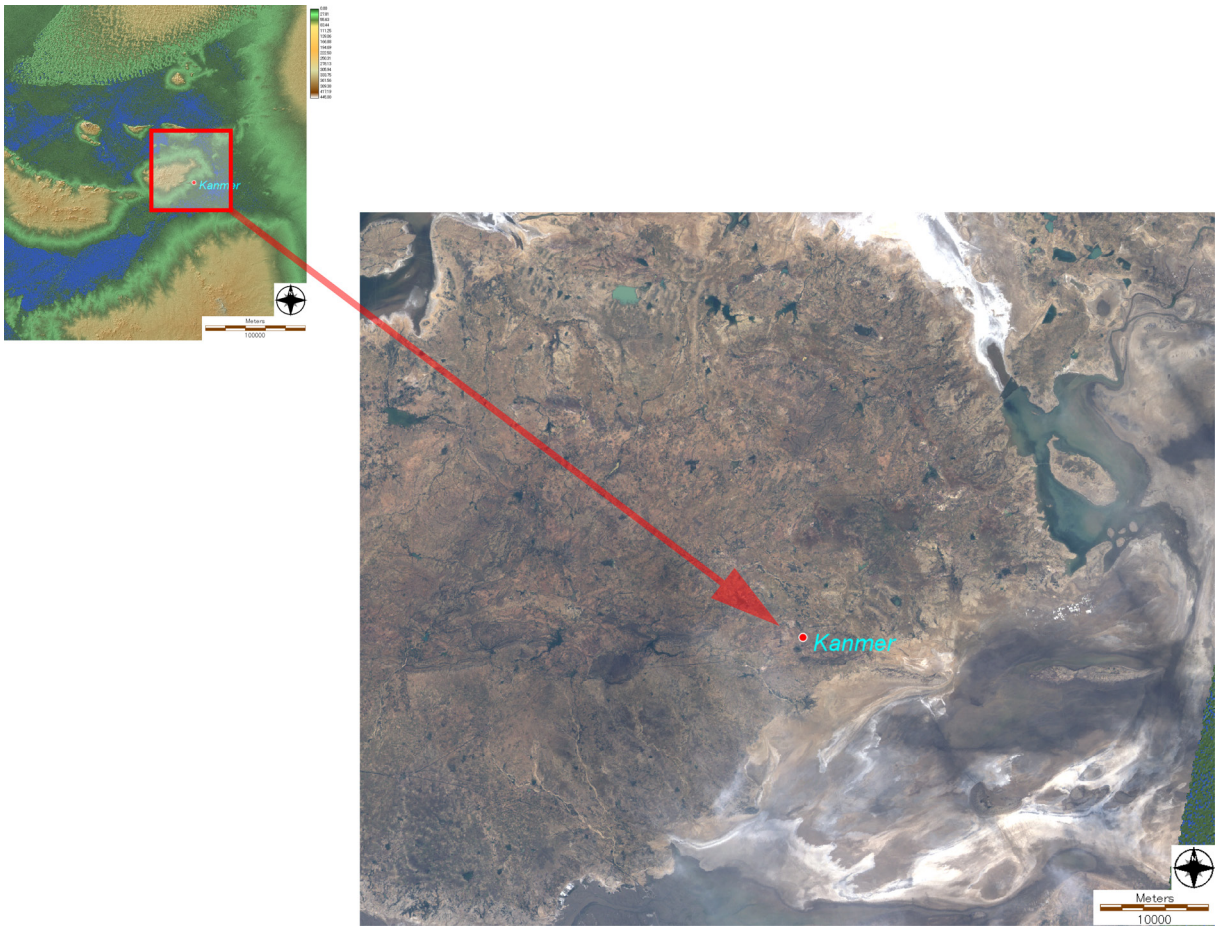

Figure 5.1.5 Location of Kanmer and Landsat imagery of the surrounding area

Gujarat (section 7). Third, for the target sites, the digital topographic survey and photogrammetry using GPS receiver and Total Station are conducted at Farmana and Kanmer in order to scan the topography of the site and its periphery as well as the intra-site structures. In addition, the quantitative data of artifacts is analyzed per spatial unit (locus or architectural structure). The final goal of the research is to integrate all the information at these three scales into GIS to suggest a new model of archaeological research system.

3. Topographic Survey

The Harappan site of Kanmer is located at the peninsula between the Great Rann and the Little Rann of Kachchh in the state of Gujarat, India. As seen in the satellite imagery (Figure 5.1.5), the occupation is settled at the proximity of the Rann to the south. Topographic survey at Kanmer was first conducted in February 2006 by Uno, positioning his own walking tracks with a pair of high-precision GPS receivers (Topcon GB500 and Trimble Pro XH). However, the DEM created from the data of this season is rather rough for several reasons. First, the walking with GPS was sometimes interrupted by the dense bush and sharp spikes of the plants. Second, Trimble Pro XH is a single frequency GPS and thus the vertical accuracy ranges from a half to one meter. In order to revise the DEM, the citadel was surveyed again by Total Station (Trimble S6) in February 2008. The survey team consisted of two to four engineers, helped by local workmen cutting spiked branches. Data points were arbitrarily placed at approximately 5m interval on the flat area and 0.5

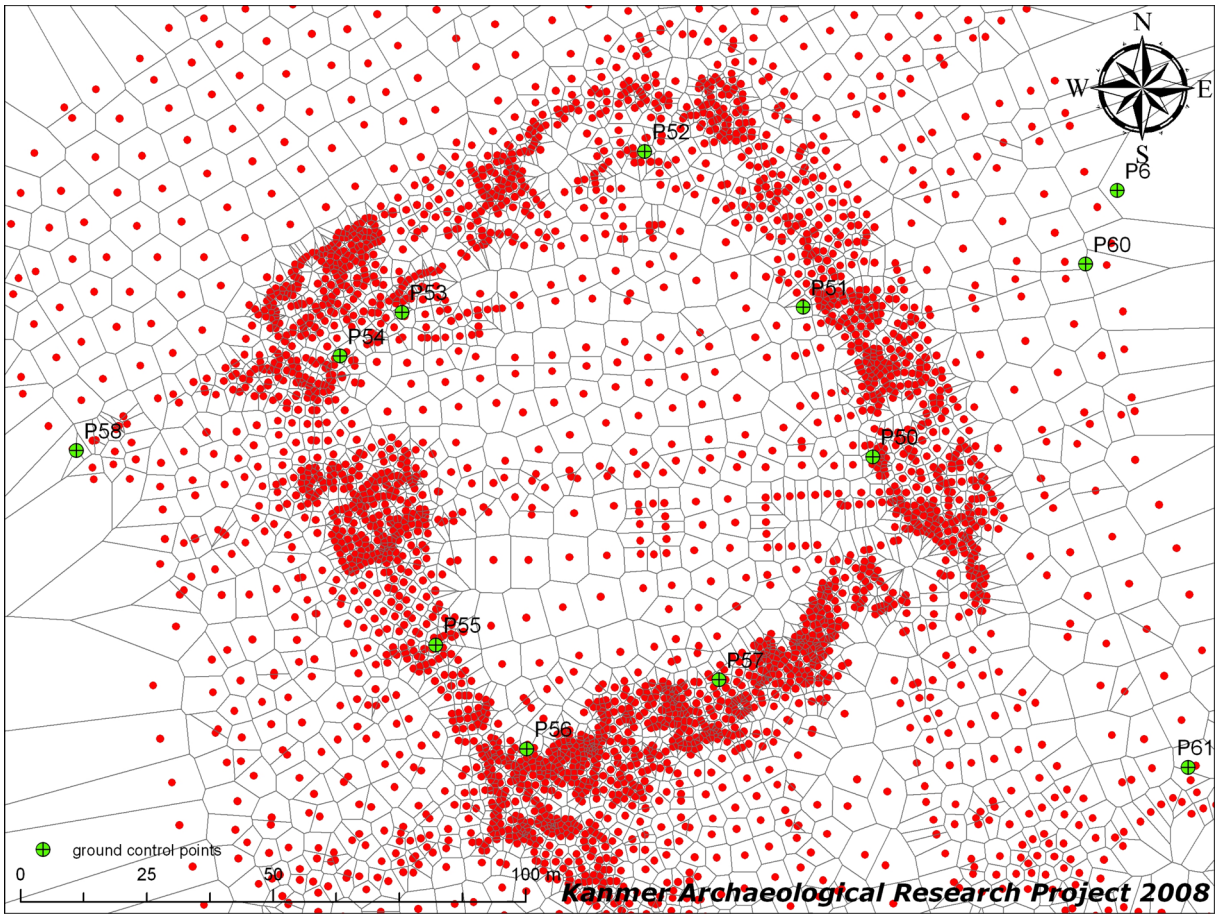

Figure 5.1.6 Data points at the citadel and the surrounding area at Kanmer

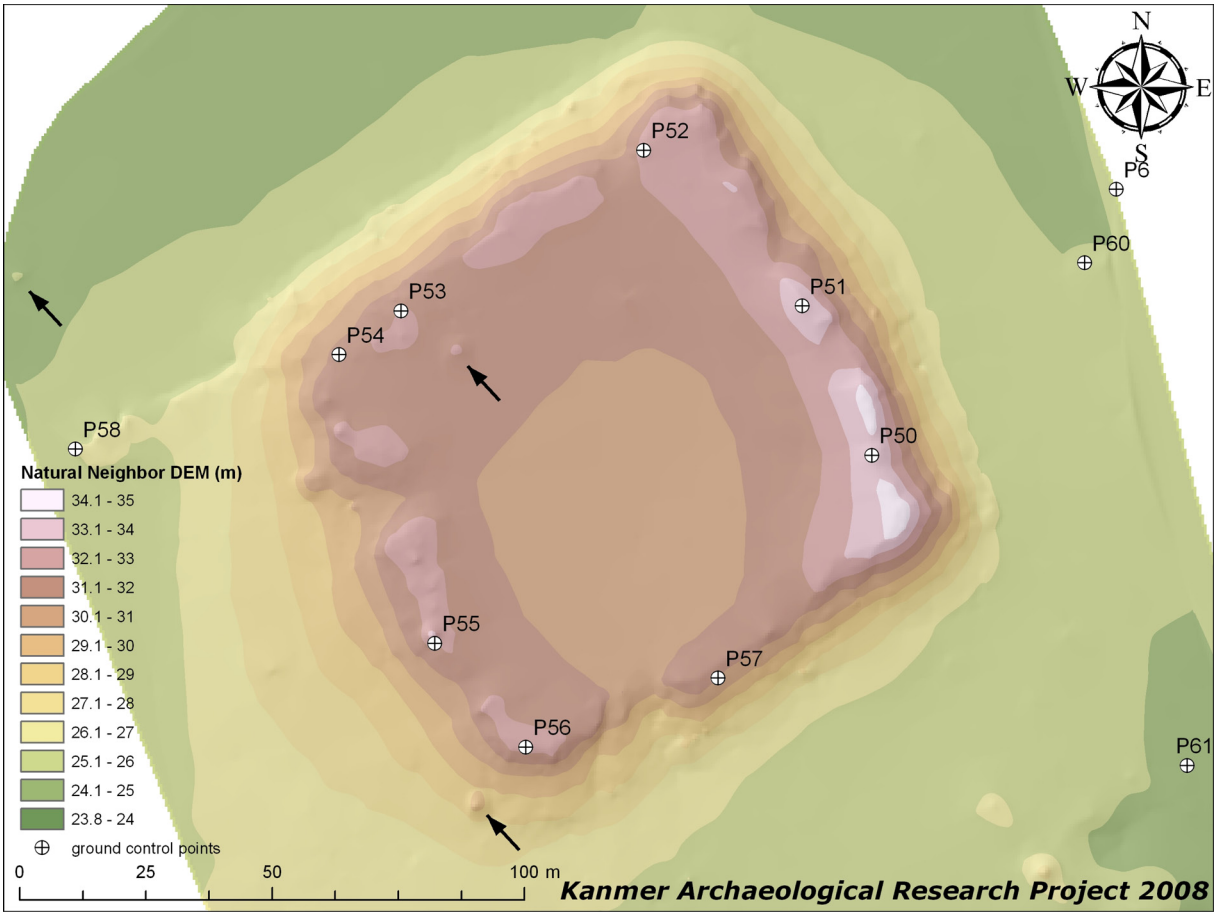

Figure 5.1.7 0.5m-grid DEM of the citadel and the surrounding area at Kanmer

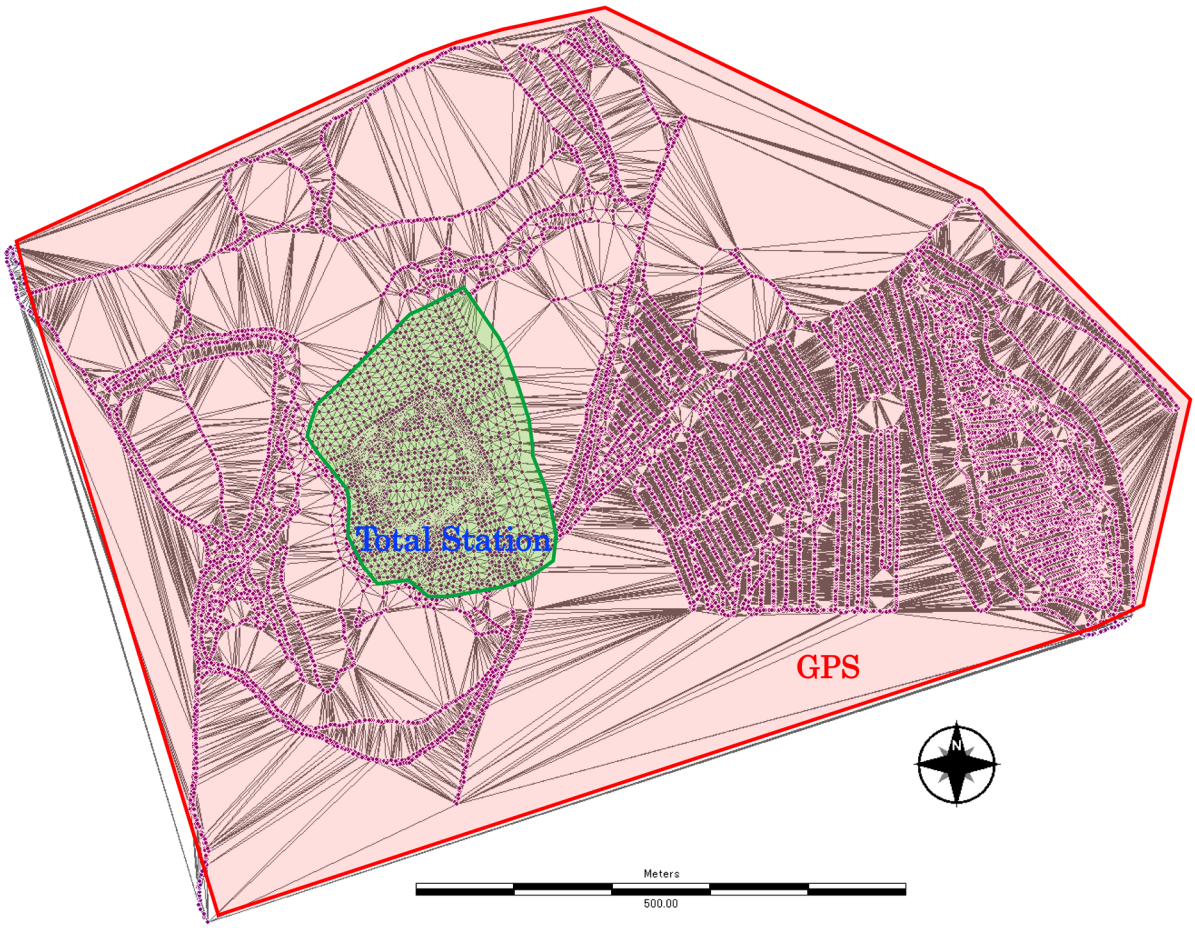

Figure 5.1.8 Survey area of the GPS and Total Station at Kanmer

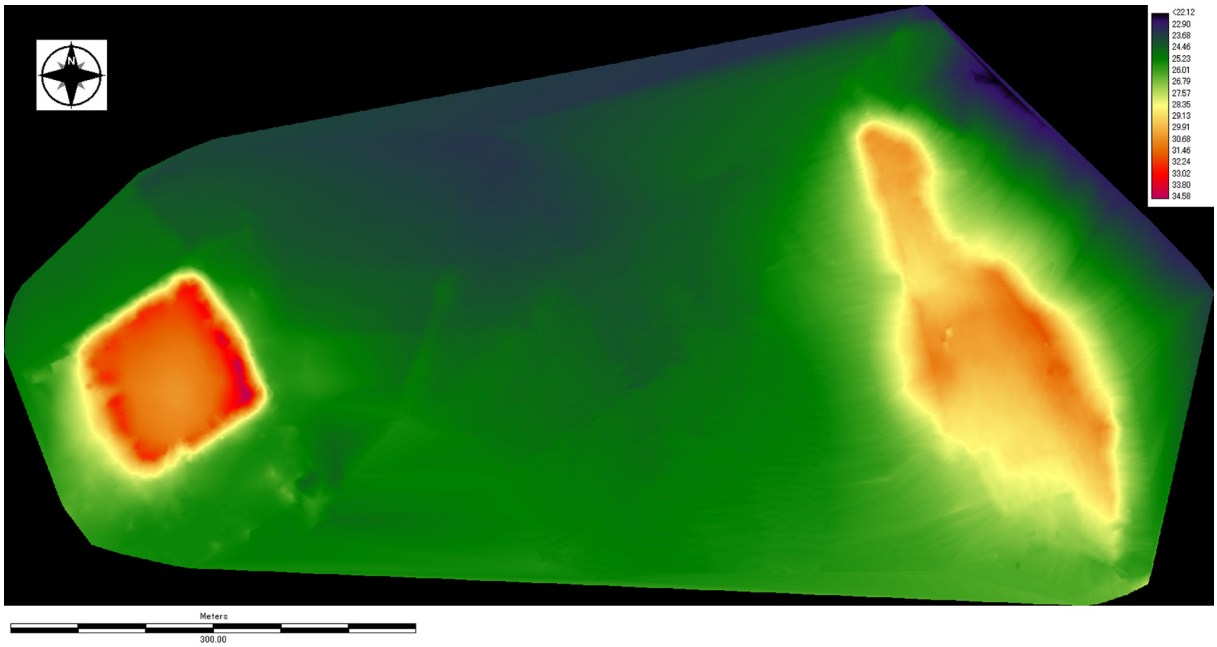

Figure 5.1.9 DEM of Kanmer (citadel) and the eastern hill (Kanmer East)

m interval on the slope. In addition, the peripheral areas, including the artifact scatter discovered on the hill in the east of the citadel, were surveyed by a pair of dual frequency GPS receivers (Topcon GB1000).

As in Kanmer, a high-resolution DEM of the citadel located at the center of the site was created by ArcGIS. The mean value of the superficial

measure of effective polygons, selected by the condition that the outermost polygons are omitted from the Voronoi polygons derived from 3,961 effective data points, is 4.5565 ㎡. The square root of this value, 2.3146, is relevant to the approximate effective resolution of the topographic survey. Based on this information, the cell size of a DEM was configured to 0.5m, approximately one fourth of the estimated resolution, and the Natural Neighbor was selected for interpolation (Figure 5.1.6 and 5.1.7).

The DEM indicates that the eastern edge of the top of the citadel mound is 1 to 2m higher than the western edge and that there are small depressions in the southern and western edges. Three "small rises" pointed by the arrows in Figure 5.1.7 should be mentioned here as a technical problem. These are aberrant values, ca. 50cm higher than the neighboring points, derived from the error occurred in the measurement: The antenna in moving might be measured. This kind of error is easily detected in the flat area because it may be represented by a remarkable outlier, but it is rather difficult in the slope. It is also very hard to keep a pin pole with prism standing still vertically on the slope, especially in the bush of spiked plants such as acacia. Therefore it is noted that the "high-precision" DEM created as a result of the topographic survey at the citadel may subliminally contain such a human error.

Figures 5.1.8 and 5.1.9 show the IDRISI-based DEMs into which the data points of the Kanmer citadel and its peripheral areas are integrated. The interpolated surface is relatively smooth although there are some missing areas between the citadel and the eastern hill (Kanmer East). Adding several data points on these areas is required for filling the gap as future task. The eastern hill was rapidly surveyed on foot with a set of high-precision GPS receivers (a pair of Topcon GB1000) due to unforeseen discovery of the artifact scatter. However, the slope and geometry of the hill are successfully captured into the DEM. The mound is a little lower than the citadel and elongated from the northwest to southeast. Although the occupation has not yet been dated, but documentation of Kanmer East and its integration into the digital surface of the citadel area are essential for dating, which is expected to elucidate the cultural association between these two sites.

Figure 5.1.10 Taking a picture from the top of a ladder (left) and a pole (right)

4. Photogrammetry

In parallel with the topographic survey, a photogrammetric survey of the unearthed architectural remains was conducted at Kanmer. In the excavations, the Indian team has been documenting the immobile remains as paper-based drawings – architecture plans and soil profiles for example, while the Japanese team has been recording them by digital photogrammetry. Once the three-dimensional geospatial information (X, Y and Z coordinate) is appended to both analog and digital documents, the complementary data

Figure 5.1.11 Architectural remains on which ground control points are placed

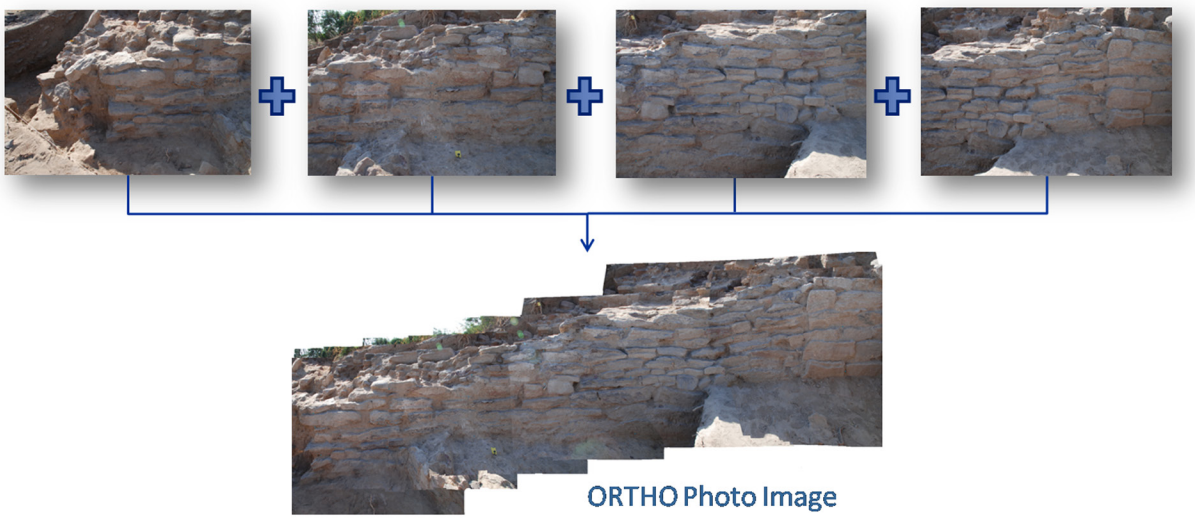

Figure 5.1.12 Process of the orthoimagery. Northeast corner of the citadel wall

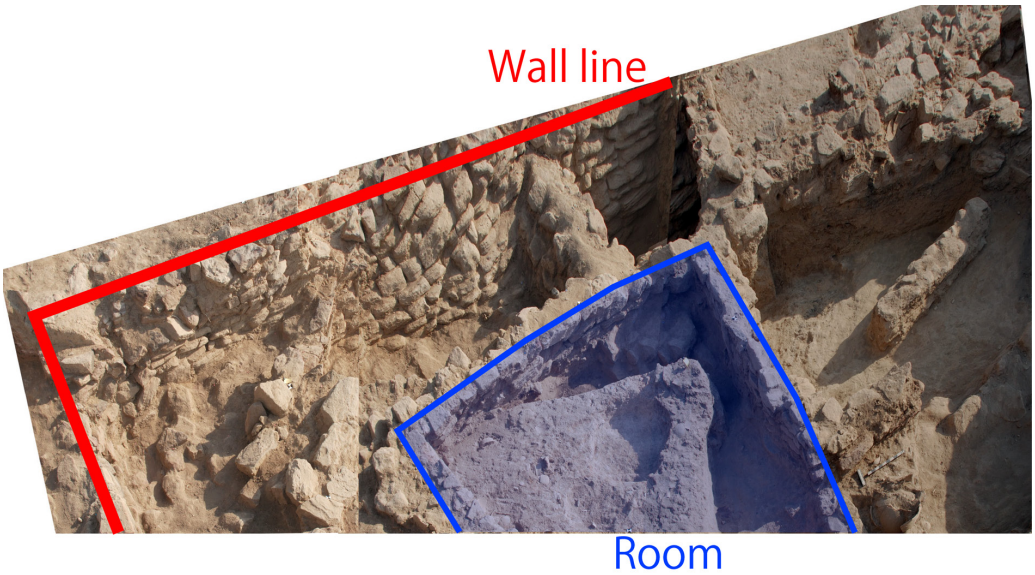

Figure 5.1.13 Orthoimagery of the architectural plan of the southeast corner of the citadel

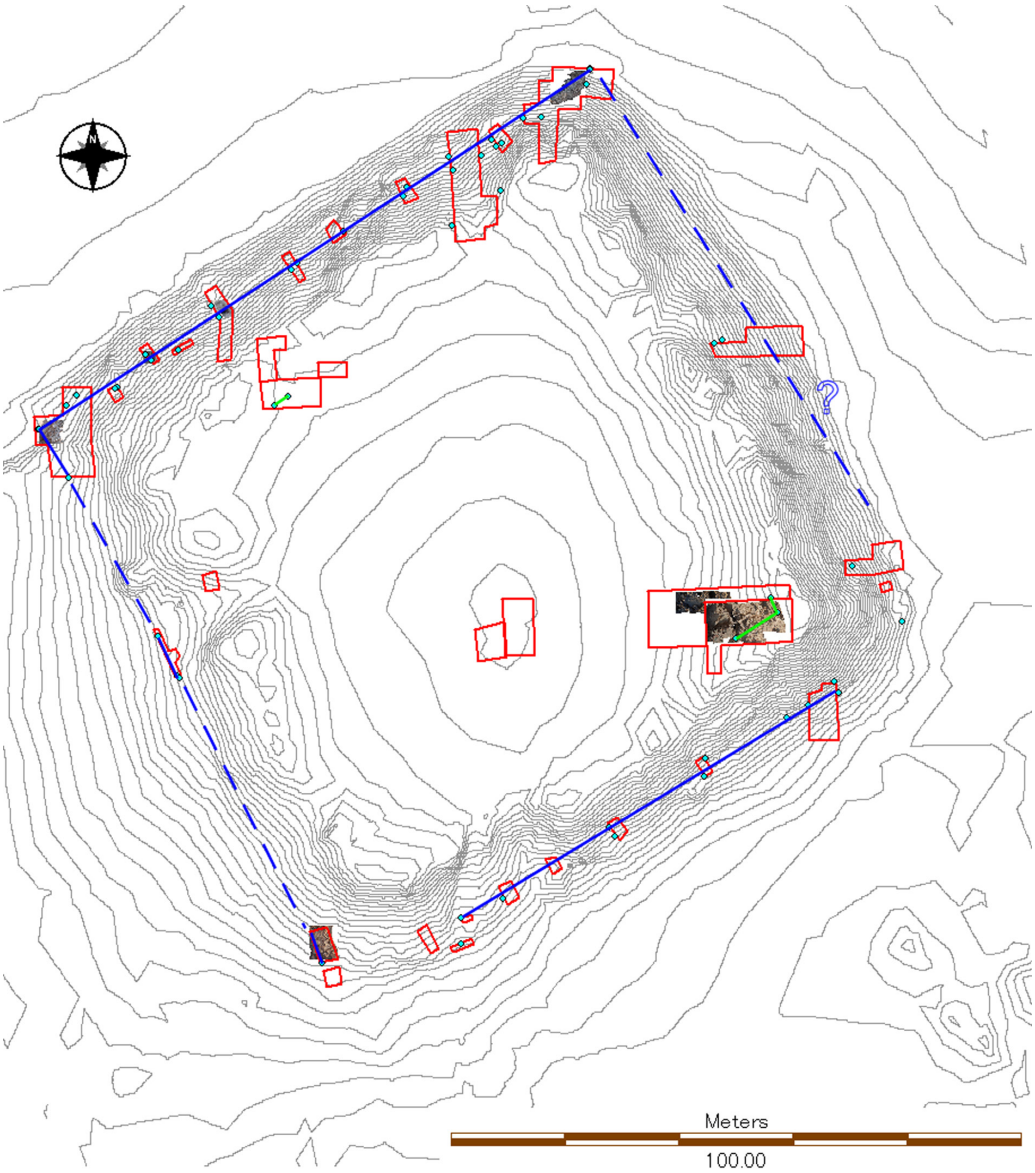

Figure 5.1.14 Overlaying the photogrammetric images on the contour map of the citadel

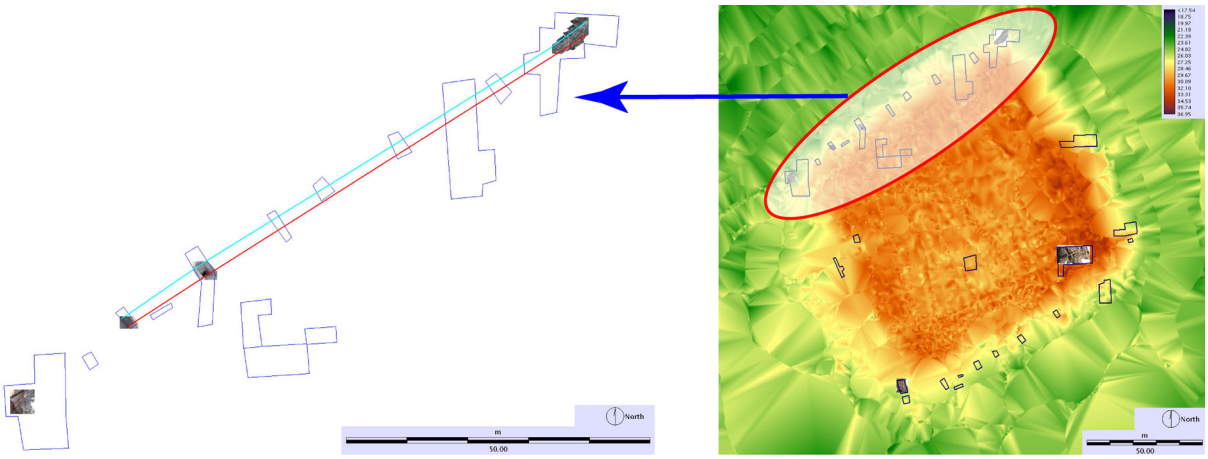

Figure 5.1.15 Reconstruction of the wall line along the north side of the citadel

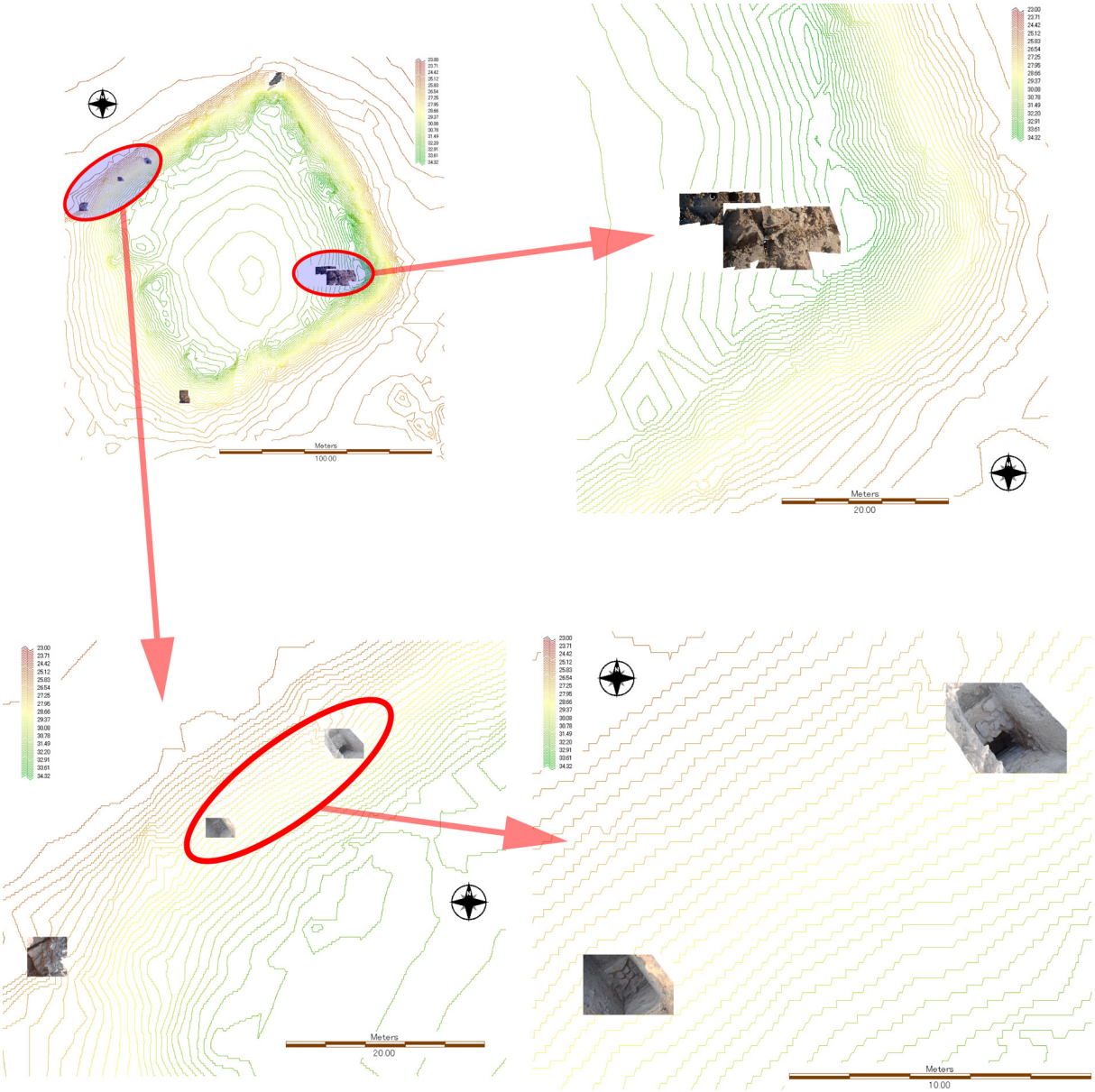

Figure 5.1.16 Overlaying the results of photogrammetry on contours

(Eastern wall)

(Northern wall)

Figure 5.1.17 Orthoimagery of the surrounding wall of the citadel

exchange will become really possible.

The first step of photogrammetry is to take a series of pictures of architectural remains or a section of sounding trench on target by means of high-end digital single-lens reflex camera (Nikon D80). Wide trench is photographed in several divisions. Section profile and elevation surface are recorded from the horizontal position, while flat architectural remains are photographed from the plumb-bob vertical position, in appropriate distance. In the first season, the photographs of the architecture plan were taken from the top of ladder, but the vertical angle was usually oblique, which caused many errors when creating an orthoimagery (Figure 5.1.10; left). For improvement, in the second season, the photos were taken from the plumb-bob vertical angle with the camera attached on the distal end of a long pole and shuttered by self-timer (Figure 5.1.10; right). Nine and more markers, functioned as ground control points, should be placed in grid pattern on the target area of photogrammetry (Figure 5.1.11). The X, Y and Z coordinate of the control points are determined by means of Total Station (Topcon GPT-9005A for the first season and Trimble S6 for the second season) to match a stereo pair of pictures on the computer.

Figure 5.1.12 displays the process of the orthoimagery, exemplified by the elevation surface of the northeast corner of the citadel wall. A pair of the georefecenced pictures, neighboring each other, is stereo-matched by means of orthoimagery application software (Topcon PI3000). This job is multiply repeated to make an orthoiamgery of the complete scene. If an elevation drawing of the stone wall is required for excavation reports, it will be possible to prepare a digital drawing by tracing the break lines in the digital illustration software such as Adobe Illustrator. Figure 5.1.13 is an orthoimagery of the architectural remains inside the southeast corner of the citadel wall. The original version of the photograph was taken from the ladder. Nevertheless, it is successful to distinguish the spatial relationship between the outer wall and a room block inside it.

The geospatial information of the ground control points photographed with architectural remains enables us to overlay the orthoimagery on the DEM in a GIS application. At Kanmer, photogrammetry has been carried out for the architectural plan of the northeast, northwest and southwest corners, the plan and elevation of the stone wall recovered in a series of sondages in the northern side, and the plan and section of the deep

sounding opened at the center of the citadel. When the orthoimageries of architecture and the location of trenches are overlaid on the contour map (Figure 5.1.14, 15 and 16), spatial relationship between the trenches and overlap/continuity of the citadel wall and other structures can be very clearly understood. In fact, the continuous stone wall is reconstructed by integrating the georeferenced orthoimageries of the citadel wall found from the remote trenches. In our view, the photogrammetric surveys at Kanmer is more fruitful than expected beforehand, although there found out some technical issues including the way to keep the pole standing still so as not to wiggle the digital camera attached on the distal tip.

5. Quantitative Spatial Analysis of Artifacts: A Preliminary Approach

The traditional archaeological excavations have focused on built remains and artifacts, and hence, theoretically, GIS-aided spatial studies of archaeological sites should target both. This paper has so far dealt with the documentation of the Harappan sites and the GIS-aided spatial analyses based on the data acquired though it. However, GIS-based studies of artifacts should be further developed for an integrated research of the archaeological site as a complex of built structures and objects.

In order to put the GIS-aided artifact studies into practice, it is necessary to develop a database according to the purpose of study. The Kanmer Archaeological Research Project (KARP), directed by Professor Jeewan Singh Kharakwal, has continuously been building a suite of the artifact database. This section presents a preliminary discussion on the GIS-based artifact analysis based on this database.

When artifacts are analyzed with GIS, the following four types of information are indispensable: (1) unique serial identifier for data management, (2) qualitative/quantitative attributes of artifacts (material, shape, dimension, color, decoration, making method and technology, usage state, and other quantitative data), (3) temporal information (time periods), and (4) geospatial information (geocoordinate, depth, layer, etc.). The object database should be designed so as to contain all these data in accordance with the GIS-based approaches targeting (a) individual artifact remains, (b) small finds from a specific lot such as individual built structure or locus, (c) intra-site distribution pattern or (d) distribution pattern in a topographic unit, geopolitical region or supra-region.

The GIS-aided artifact research by the KARP primarily focuses on the intra-site spatial analysis (c). It is not only one of the most important research topics of the processual and post-processual archaeology in the second half of the 20th century, but also a research field that could be greatly innovated by GIS. It could also provide a high-quality dataset for the regional and supra-regional spatial analyses of artifacts (d).

There are many types of artifacts uncovered from archaeological sites, and the attributes to describe them differ from one to another. However, in the GIS-aided intra-site spatial analysis of artifacts, the common dataset including the qualitative/quantitative, temporal and geospatial information should be provided for each type of artifact in a realistic manner. With regard to the qualitative/quantitative information, for instance, the pottery database of the KARP contains that of fabric, forming method (handmade or wheelmade), firing state, decoration, typological classification and potsherd counts of rim, body and base (Table 5.1.1). Similarly, the small-finds database records material and object type as qualitative/quantitative information

Table 5.1.1 Specifications of the KARP potsherd inventory (courtesy of J.S. Kharakwal)

Item	Data Type	Description, Format and Examples	Information Category
Serial No.	Integer	Unique identifier.	Data Management
Trench Lot No.	String	Name of trench and excavation locus.	Spatial/Management
Layer	String	Stratigraphic context: Layer 1, 2a, 2b, 3 … n.	Spatial Data
Depth	Real	Depth from surface, in meter.	Spatial Data
Ceramic style and Cultural Period	String	Typological and periodical name.	Object Attribute
Type	String	Typological name.	Object Attribute
Weight	Real	Total weight of potsherds, in gram.	Object Attribute
Fabric	Integer	Potsherd count per the fabric sub-types: Fine, Medium or Coarse.	Object Attribute
Technology	Integer	Potsherd count per the forming technique sub-types: Fast wheel, Slow wheel or Hand-made.	Object Attribute
Firing	Integer	Potsherd count per the firing status sub-types: Uniform, Ill or Over-fired.	Object Attribute
Decoration	Integer	Potsherd count per the surface decoration sub-types: Incised, Appliqué, Painted and Others.	Object Attribute
Rim	Integer	Potsherd count of each part per the shape classifications: Jar, Pot, Bowl, Basin, Dish, Goblet, Lid, Ring/Stand or Others.	Object Attribute
Body	Integer		Object Attribute
Base	Integer		Object Attribute
Retained	Integer	Count of retained potsherds.	Object Attribute
Total	Integer	Total count of potsherds.	Object Attribute

(Table 5.1.2). The databases of faunal and floral remains are also under construction in terms of the similar scheme. As described here, the method of documentation should be schematized in each object category.

The quantitative information is essential to the GIS-aided spatial analysis of archaeological objects. The most fundamental data are number of fragments. Using numerical data, a scatter map of the objects can be created and the distribution pattern can be analyzed by GIS. However, it is more accurate to evaluate the voluminal amount of the artifacts than the simple count because of great diversity in size of fragments. In this respect, weight can directly be analyzed as quantitative data. It is also possible to estimate the number of object from the average weight of unbroken speciomens. The KARP excavation team has recorded the weight of every small find in addition to the number of fragments, and thus the amount of artifacts can be quantified per typological class, trench or layer.

At present, the temporal information is incorporated into the pottery database as relative chronology (ware and cultural period). Layer is also useful for relative chronology to attest pottery seriation and typology. In the near future, the AMS radiocarbon and other scientific dating methods will provide absolute chronology for each layer to quantify temporal information. When artifacts terminus ante quem are included in a layer, their dating will be verifiable with the attached quantitative information.

The geospatial information being attached to artifacts can accurately be defined by means of photogrammetric instrument or Total Station in the case of important finds. However, in fact, a great variety/number of artifacts, including small

Table 5.1.2 Specifications of the KARP small-finds database (courtesy of J.S. Kharakwal)

Item	Data Type	Description, Format and Examples	Information Category
Serial No.	Integer	Unique identifier.	Data Management
Date	Date	DD/MM/YYYY	Data Management
Trench	String	Trench name. FF29, GG30, etc.	Spatial Data
Quadrant	String	Quadrant of trench: NE, NW, SW and SE.	Spatial Data
Along	Real	Northing in meter.	Spatial Data
Away	Real	Easting in meter.	Spatial Data
Lot No.	Integer	Unique identifier of excavation locus.	Spatial Data
Depth	Real	Depth from surface, in meter.	Spatial Data
Layer	String	Stratigraphic context: Layer 1, 2a, 2b, 3 … n.	Spatial Data
Object	String	Name of object: blade, bead, bangle, etc.	Object Attribute
Material	String	Stone, steatite, agate, carnelian, copper, etc.	Object Attribute
Remark	String	Additional information about context or object.	Spatial/Object

and microscopic remains that can only be detected by water flotation or sieving, are unearthed from the site. Thus it is almost unrealistic to record the three-dimensional location of all these remains one by one. At Kanmer, the excavation team has set 5-m-grid trench system and recorded tetrameric portion (or 2.5-m-grid cell of the northeast, northwest, southeast or southwest quadrant) of square trench as well as layer number and depth [m] from the surface for defining locus of artifacts. Therefore, it is at least possible to attach these as the common geospatial information to all the recovered objects.

After the artifact databases including attributes, temporal and geospatial information have become available, the quantitative spatial distribution pattern of artifacts will be displayed and analyzed by GIS, overlaid on the layers of DEM or contour and architectural plan (see Figures 5.1.18 - 23). Among the artifacts, pottery is composed of various taxa such as the Harappan or local pottery in typology and the storage jar or tableware in usage. Personal ornaments are also diverse in both typology (bead, micro-bead, pendant and bangle for instance) and material (copper, carnelian, agate, steatite, faience, terracotta and shell). The quantitative spatial pattern (uniform or uneven distribution) of these objects and the spatial correlation between artifact distribution and architecture will provide interesting results. Furthermore, the comparative spatial analyses between different objects such as stamp seals, stone industry tools, faunal and floral remains will contribute to understand their economic and symbolic values. These are fundamental approaches of the GIS-based artifact studies targeting the site, and therefore we will be conducting these studies continuously.

As the final part to this section, the authors would like to put “the digital approach to an individual object” in proper perspective (a). For the moment, it is still unrealistic to make it operational for technical and temporal restrictions. However, in the future, this kind of detailed data will provide a higher-quality solution for other approaches at different analytical scales (b, c and d).

The elemental job of the digital studies of artifacts is not to describe and document the attributes but to construct digitalized data. The

Minor object Database & Vector file (Grid)

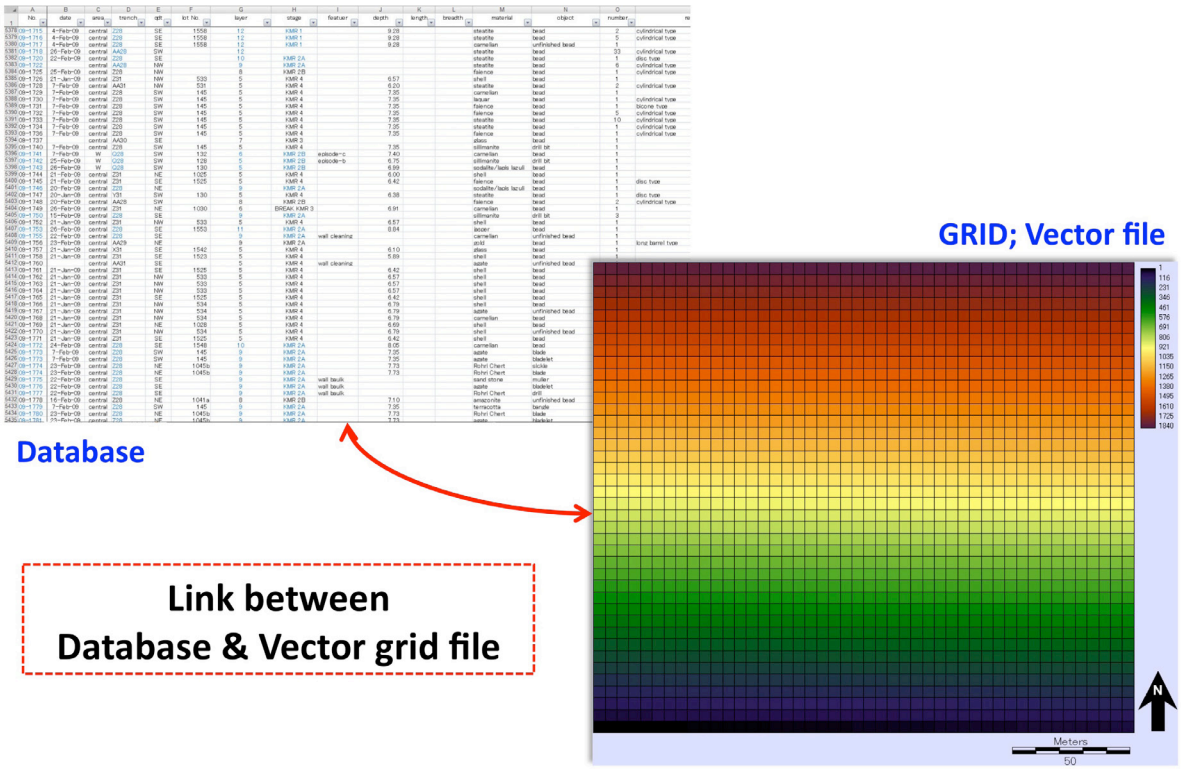

Figure 5.1.18 Database & Vector file

Distribution of All minor objects

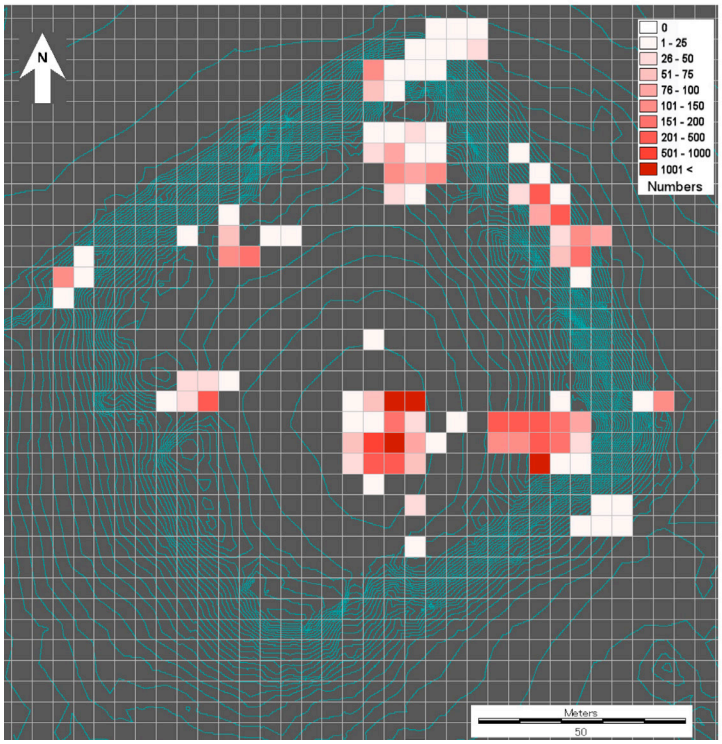

N=23,680

Numbers per 5m×5m Grid

(Include unknown layer objects)

Legend	Numbers
0	0
1	1 – 25
2	26 – 50
3	51 – 75
4	76 – 100
5	101 – 150
6	151 – 200
7	201 – 500
8	501 – 1,000
9	> 1,001

Figure 5.1.19 Distribution of all minor objects

KANMER (KMR) : Cultural Periods

Cultural Periods	
KMR Ⅰ	: Pre Fortification
KMR ⅡA	: Urban
KMR ⅡB	: Urban (with new elements)
KMR Ⅲ	: Post urban
KMR Ⅳ	: Historic
KMR Ⅴ	: Medieval

(by courtesy of Dr. J. S. Khrakwal)

・Total number of the minor objects

Periods	KMR Ⅰ	KMR ⅡA	KMR ⅡB	KMR Ⅲ	KMR Ⅳ	KMR Ⅴ	Total
Numbers	873	2654	1475	13919 (2157)	1834.5	518.5	21,274

(11,762=Steatite beads)

(Layer : KMR Ⅳ/Ⅴ mixed → Divided by 2)

Figure 5.1.20 Cultural periods of Kanmer

shape and profile of an object can be modeled from the data points with local X, Y and Z coordinate supplied by three-dimensional laser scanner. Data points in 0.1-mm-interval or higher resolution would enable us to digitalize not only the complete figure of an artifact but also more detailed information such as forming method, surface treatment and use wear. In the case of an in situ object, determination of at least three control points on its surface based on the geocoordinate system, which is also applied to the topographic and architectural survey, will allow to convert the local coordinate of the data points of artifact into the geocoordinate used in the fieldwork. This will enable the GIS-aided spatial analysis of artifacts in association with the geospatial information on their provenance.

When the geometry of an object is overlaid by the information about color and decoration as a texture, all the digital information recorded in the form of drawing and photograph has been incorporated into a suit of digital data with geospatial reference. At present, attaching a digital imagery calibrated by the standard color chart to the three-dimensional framework of the same object provides the highest-precision digital model. It is expected in the future that data of color and decoration will be simultaneously acquired by laser scanning of the shape.

Ideally, the data of artifacts contained in GIS should include all the information required for artifact studies. The qualitative/quantitative information is used for typological studies of artifacts and the geospatial information contributes to stratigraphical studies. Since the positional data also provide the information on the direction and angle of objects in the deposit, it is also useful to reconstruct the artificial/natural depositional process of the site and artifacts from the viewpoint of geoarchaeology.

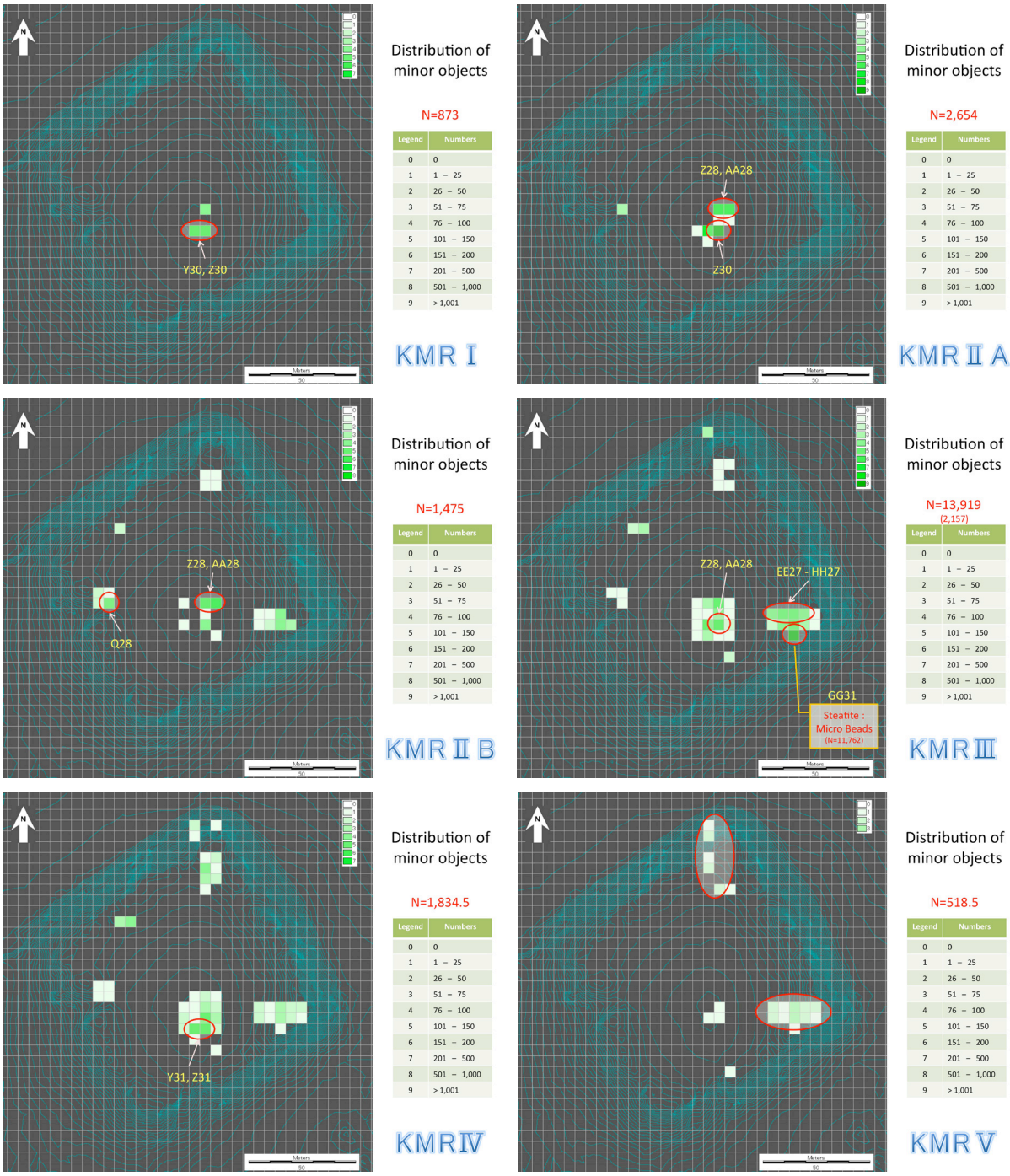

Figure 5.1.21 Diachronic changes of the distribution of minor objects

It is also noteworthy that not a little amount of quantitative information can automatically be acquired from the GIS-oriented database. For example, the total weight of artifact fragments can be calculated from individual gravity and volume, and the total number of individual objects can be estimated from distinctive fragments such as rim of pottery or distal tip of lithic tools. In the future, information for helping reconstruction of fragmented artifacts will also be provided by these studies.

The digital-oriented artifact studies at Kanmer are currently conducted as a pilot study, and they have not yet been suitable for practical operation due to much time and labor required for data mining and processing as well as provisionally gigantic volume of digital data. However, in the near future, practical application of the laser

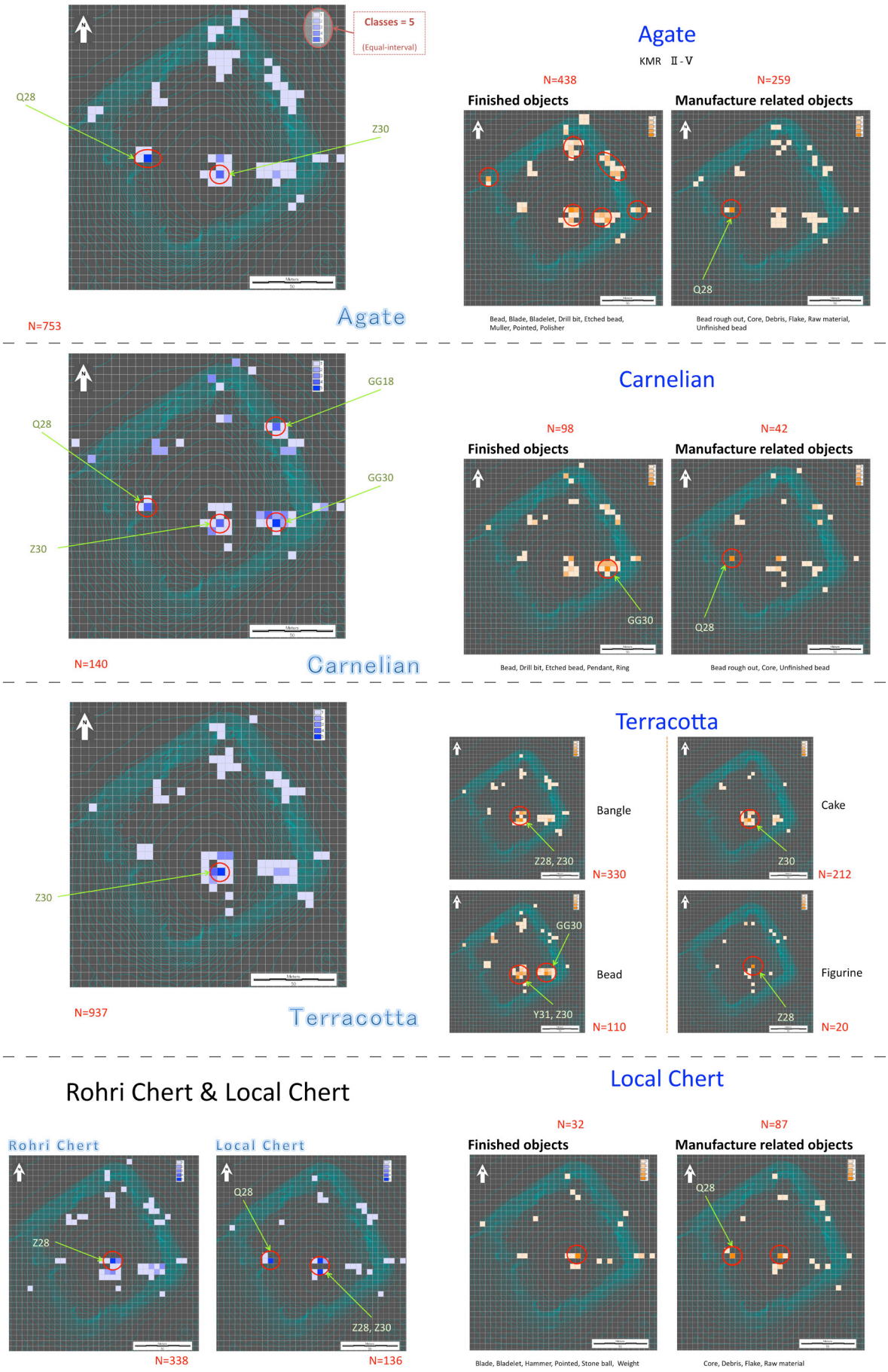

Figure 5.1.22 Distribution of minor objects ①

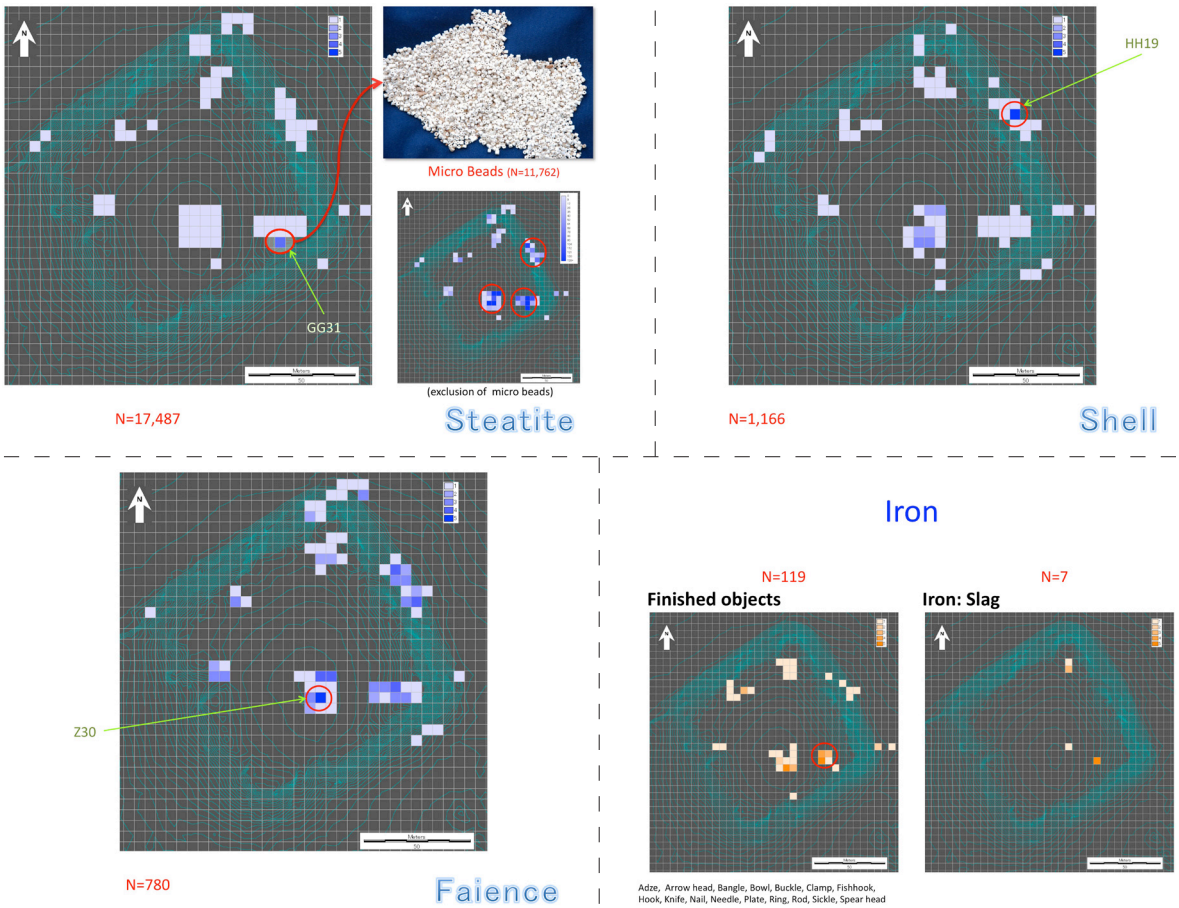

Figure 5.1.23 Distribution of minor objects ②

scanning technology that is able to search and distinguish artifacts in situ from structural remains will serve for laborsaving. Our future task at Kanmer is to make the GIS-oriented research of artifacts into a fully operational system after taking account of all contentious technical issues.

6. '3D Modeling' of Artifacts

We tried creating 3D models of artifacts such as Indus seals, pendants with seal impression, sealings and sherds with incised motif using 3D Laser scanner. The purpose of 3D modeling of artifacts is developing of Digital Archive of cultural properties based on applying digital technology in archaeology.

We used PICZA – LPX-1200 (3D Laser scanner supplied by Roland Co.) to collect XYZ coordinate values of points on surface of artifacts (Figure 5.1.24). Minimum pitch of points which PICZA – LPX-1200 could collect is 0.1mm, and the machine could work without touching artifacts.

We created polygon-meshes by processing collected coordinate values of points on computer, and it enable to digital documentation of each artifacts (Figure 5.1.25). Furthermore we created 3D models of artifacts by interpolating polygon-meshes using modeling software. We say the process of lapping of surface of polygon-meshes and displaying 3D models of artifacts as 3D modeling (Figure 5.1.26). Created 3D models are represented as 2D image on display of computer, but we could rotate, zoom in/ out or observe from any directions on display using 3D rendering technology.

Figures 5.1.27 - 29 show terracotta pendants

Figure 5.1.24 Roland PICZA (LPX-1200)
(Left: External appearance, Center: Inside of the machine, Right: Turntable)

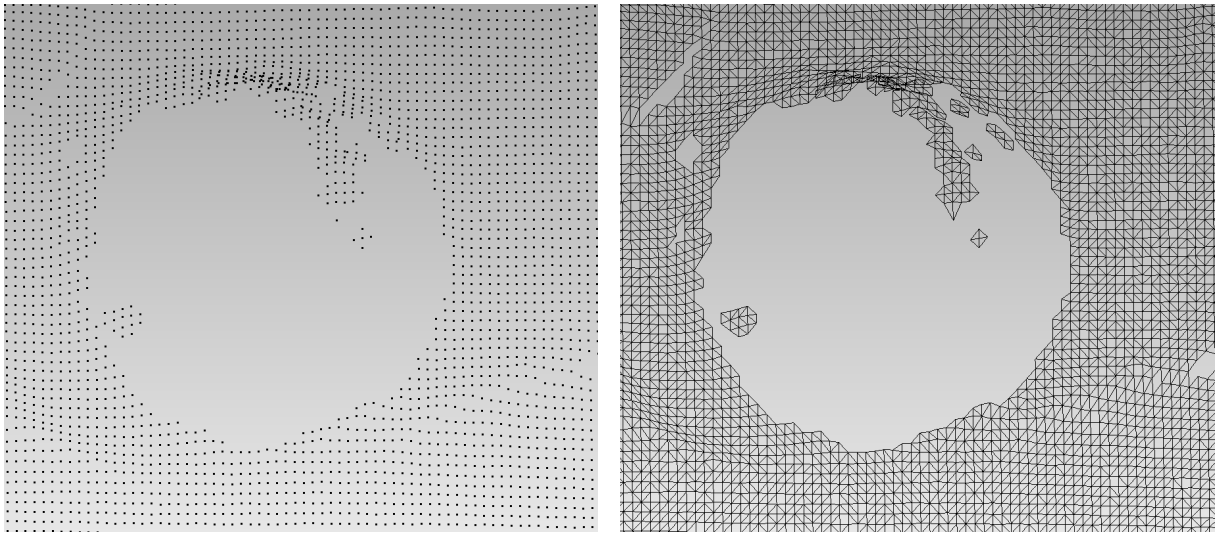

Figure 5.1.25 Point (Left) & Polygon mesh (Right)

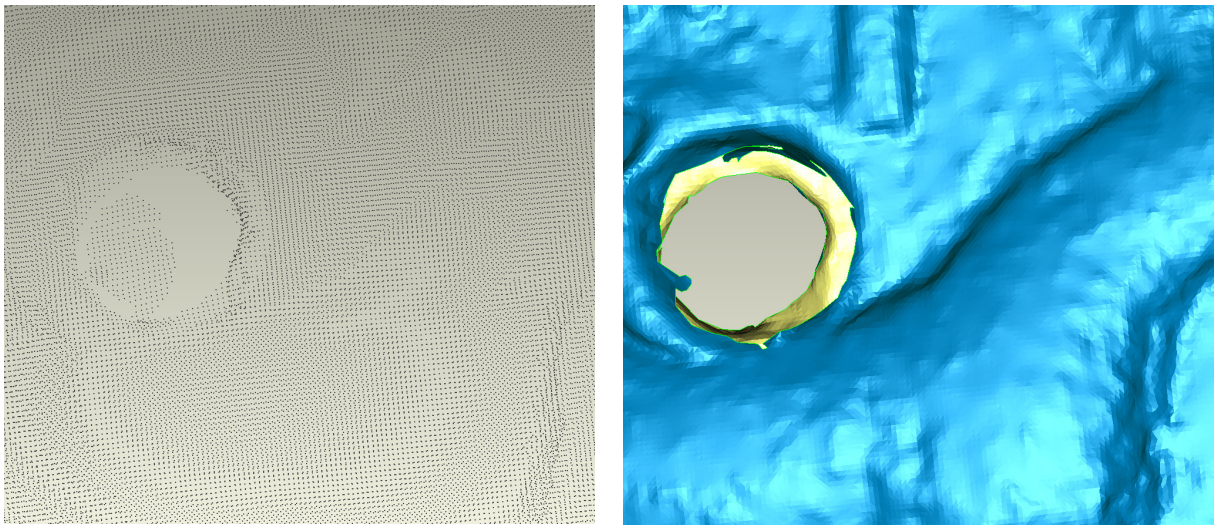

Figure 5.1.26 Point (Left) & Wrap surface [3D model] (Right)

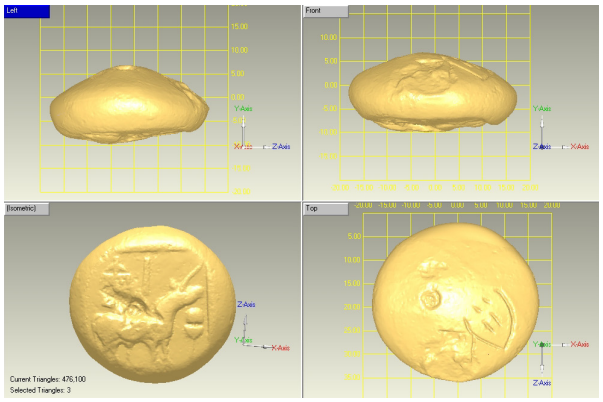

Figure 5.1.27 Seal impression (899c)

Figure 5.1.28 Seal impression (900c)

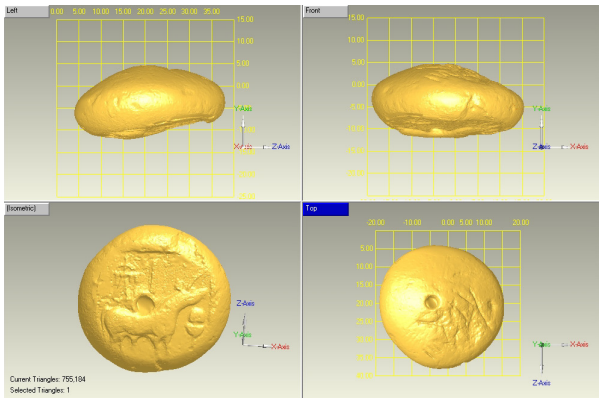

Figure 5.1.29 Seal impression (1286b)

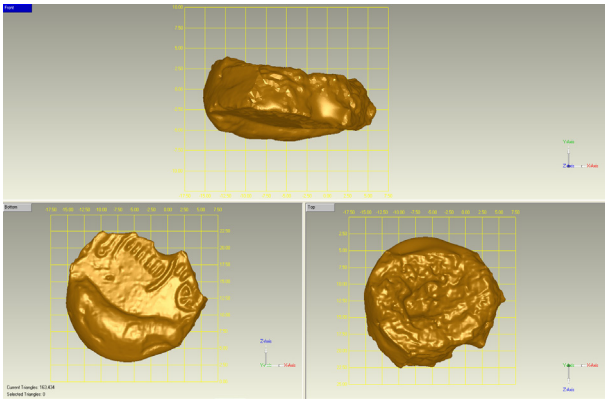

Figure 5.1.30 Sealing (1054)

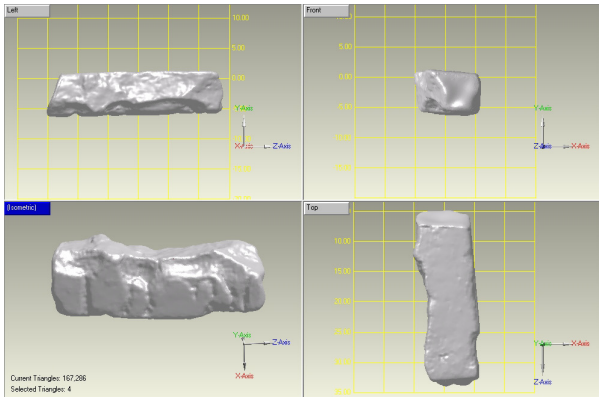

Figure 5.1.31 Seal (1996c)

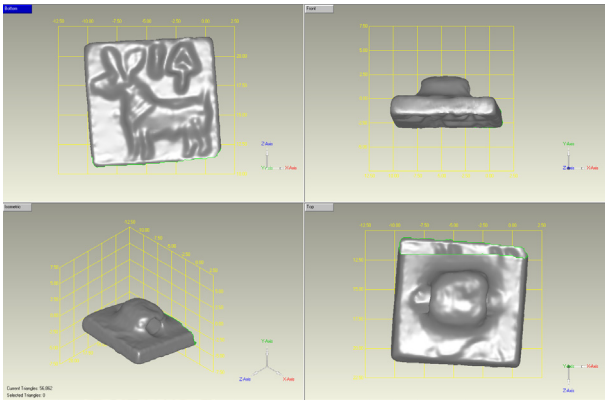

Figure 5.1.32 Seal (1997c)

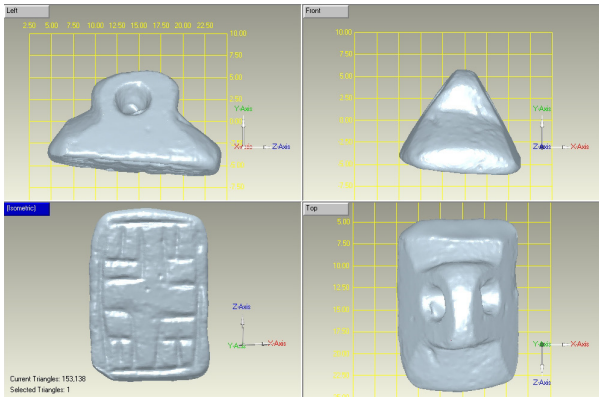

Figure 5.1.33 Seal (1995c)

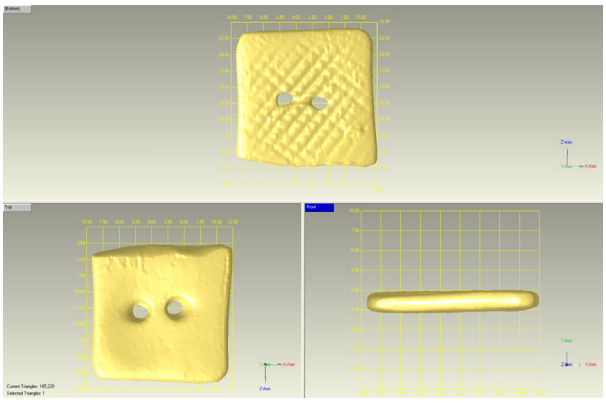

Figure 5.1.34 Seal (1007)

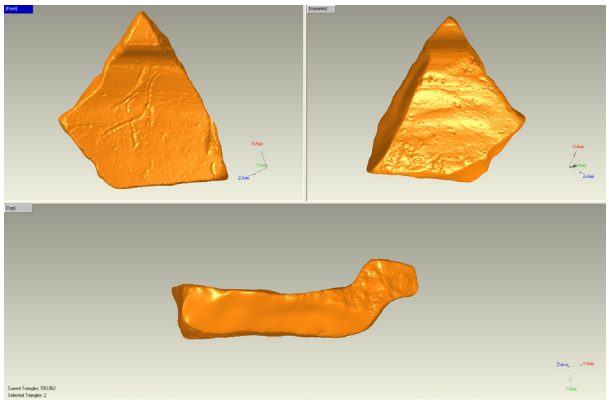

Figure 5.1.35 Engraved Pottery (1203c)

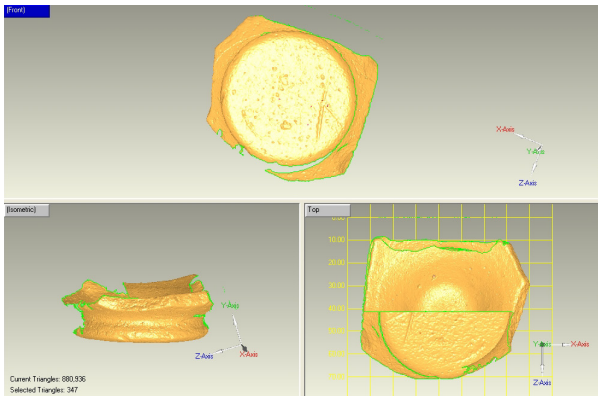

Figure 5.1.36 Engraved Pottery (158g)

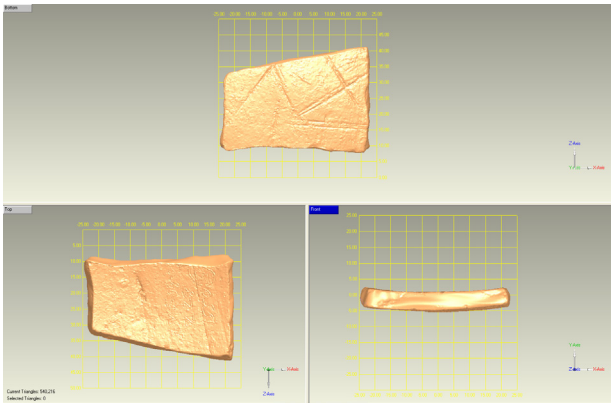

Figure 5.1.37 Engraved Pottery (1550)

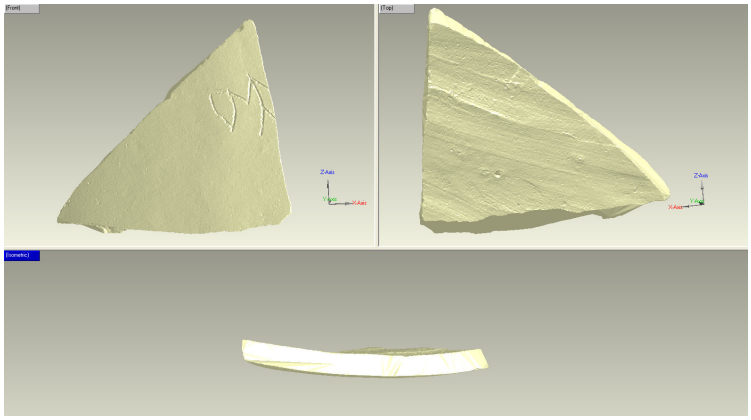

Figure 5.1.38 Engraved Pottery (1285b)

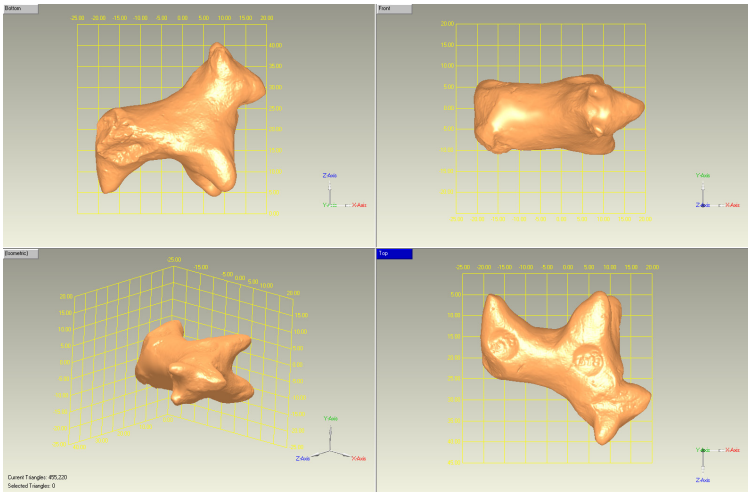

Figure 5.1.39 Figurine (530b)

baked after stamping by Indus seals and perforating. Figure 5.1.30 shows chipped sealing which stamped by Indus seals. Figures 5.1.31 - 34 show Indus seals incised geometric or animal motif. Figures 5.1.35 - 38 show sherds of pottery with incised motif, and motif is clear because we collected coordinate values of points on surface of sherds in 0.1mm pitch. Figure 5.1.39 shows animal terracotta.

7. Distribution of the Harappan Sites

Aims of the Analysis

As described in the methodological section, the supra-regional and regional level spatial analyses aim at understanding the diachronic change of the spatial distribution of the Harappan urban settlements, paying special attention to the association between the site location and the natural settings such as topography, river course and sea level change. This will contribute to clarify the dynamism of the civilization.

Data Sources and Method of the Analysis

The spatial analysis in this section is preceded by preparating the database of the Harappan-related settlements and the supra-regional DEM covering the entire South Asia.

First of all, the fundamental data of the Harappan-related sites were imported into the geodatabase from the earlier version published by Gregory Possehl (Possehl 1999). The data includes toponym, geodetic location (latitude and longitude), time periods and superficial measure of the sites. 2,020 Harappan-related sites, which are clearly georeferenced and dated, have been selected to our database, out of 2,502 sites recorded by Possehl (Ibid.). Following his chronological scheme, time periods are subdivided into seven stages (Table 5.1.3). Multi-period sites are counted at each stage.

Second, supra-regional and regional DEMs were created from the SRTM-3 (Shuttle Radar Topography Mission; ca. 90-m-mesh resolution) and SRTM-30 (ca. 1-km-mesh) provided by NASA. These raster data were imported to IDRISI by the agency of GISmap, free data-management software developed by Izumi Niiro. The recorded sites were then plotted on the DEM to conduct runoff, density distribution, viewshed and sea level change analyses by IDRISI.

Figure 5.1.40 shows archaeological sites in the study area plotted on the DEM. The area of distribution covers the Balochistan Hills to the west, the Upper Ganges Valley to the east, and the Saurashtra Peninsula to the south. In order to examine diachronic change of the site distribution, the site density of each chronological stage has been analyzed (Figure 5.1.41). In the density maps, the darker (blue-colored) zone indicates the higher site density. At Stage 1, a dense cluster of archaeological sites is observed in and around the Balochistan Hills. At Stage 2, in addition to this region, the Middle Indus Valley gets densely occupied. Furthermore, at Stage 3, the distribution expands to the east, and another site cluster is observed in the Upper Ganges Valley. Stage 4 is characterized by the relatively sparse site distribution and appearance of sites in the Gujarat region in the south. Stage 5 shows a dramatic increase of sites, particularly in the Saurashtra Peninsula. There are also three high-density areas – Gujarat, the Middle Indus and the Upper Ganges, as well as a smaller cluster in the Balochistan Hills. The density distribution of Stage 6 is polarized into the larger cluster in the Upper Ganges and the smaller in Gujarat. At the final phase, Stage 7, sites appeared only in the Upper Ganges, and not in the Middle Indus, the Saurashtra Peninsula and the Balochistan Hills.

Figure 5.1.42 indicates the possible river

Table 5.1.3 Chronological table of Indus civilization (after Possehl 1999)

Stage 1	7000-5000 BC 5000-4300 BC	Beginnings of village farming communities and pastoral camps
Stage 2	4300-3800 BC 3800-3200 BC	Developed village farming communities and pastoral societies
Stage 3	3200-2600 BC	Early Harappan
Stage 4	2600-2500 BC	The Transition of Early and Mature Harappan
Stage 5	2500-1900 BC	Mature Harappan
Stage 6	1900-1000 BC	Post-urban Harappan
Stage 7	1000-600 BC	Early Iron Age

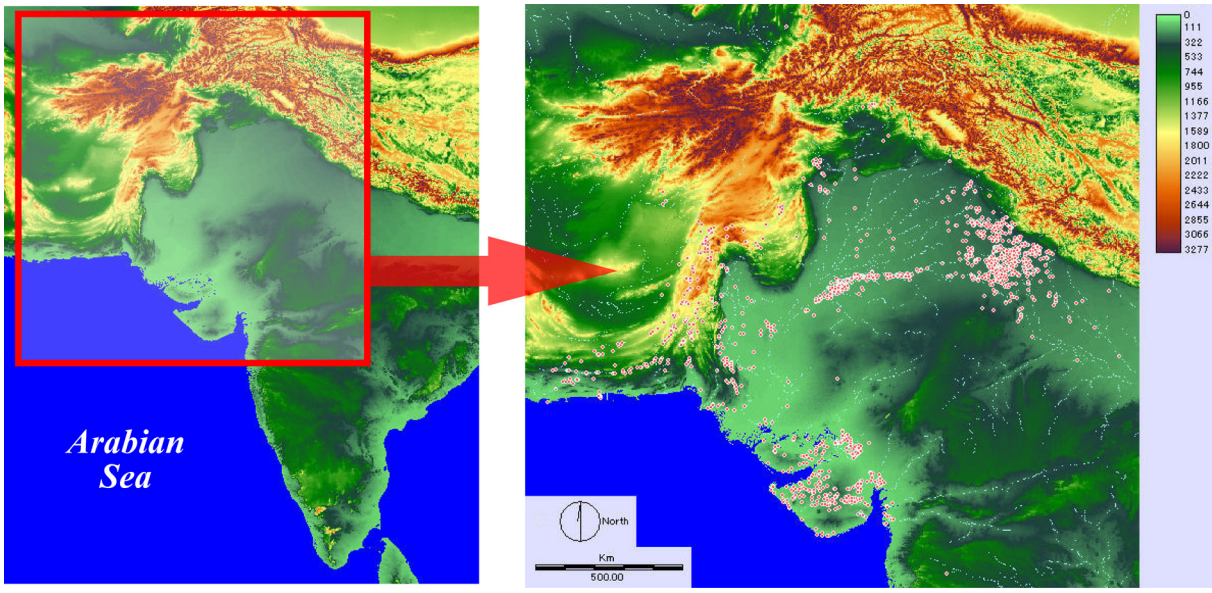

Figure 5.1.40 DEM and distribution of archaeological settlements of the study area (all stages)

passages (in ca. 1-km-mesh resolution) in the study area, simulated by the Run-off module of IDRISI. The analysis predicts a river running southeast through the currently dried-up riverbed located in the east of the Middle Indus Valley. It is probably corresponding to the ancient Ghaggar-Hakra river, but a more detailed analysis with a higher-resolution DEM is strongly required for attesting this interpretation.

The viewshed analysis helps us to understand the location of the Harappan "mega-sites", such as Harappa, Mohenjo-daro and Dholavira, from the aspect of landscape visibility (Figure 5.1.43). The visible areas from Harappa and Mohenjo-daro suggest that these sites are located at a focal point so that the upper (for the former) or the lower Indus Valley (for the latter) can be in sight. Although Mohenjo-daro and the Gujarat sites are too remote to be seen from each other, but there is theoretically no "viewshed barrier" between these two groups.

Harappan Sites in Gujarat

In the regional scale, archaeological sites in the northern part of the Saurashtra Peninsula and the Rann of Kuchchh region are plotted on the DEM (Figure 5.1.44; Dholavira and Kanmer are indicated as star symbol). The Rann of Kuchchh is a salt marsh that is filled by water in the rainy season and almost dried-up in the dry season. The

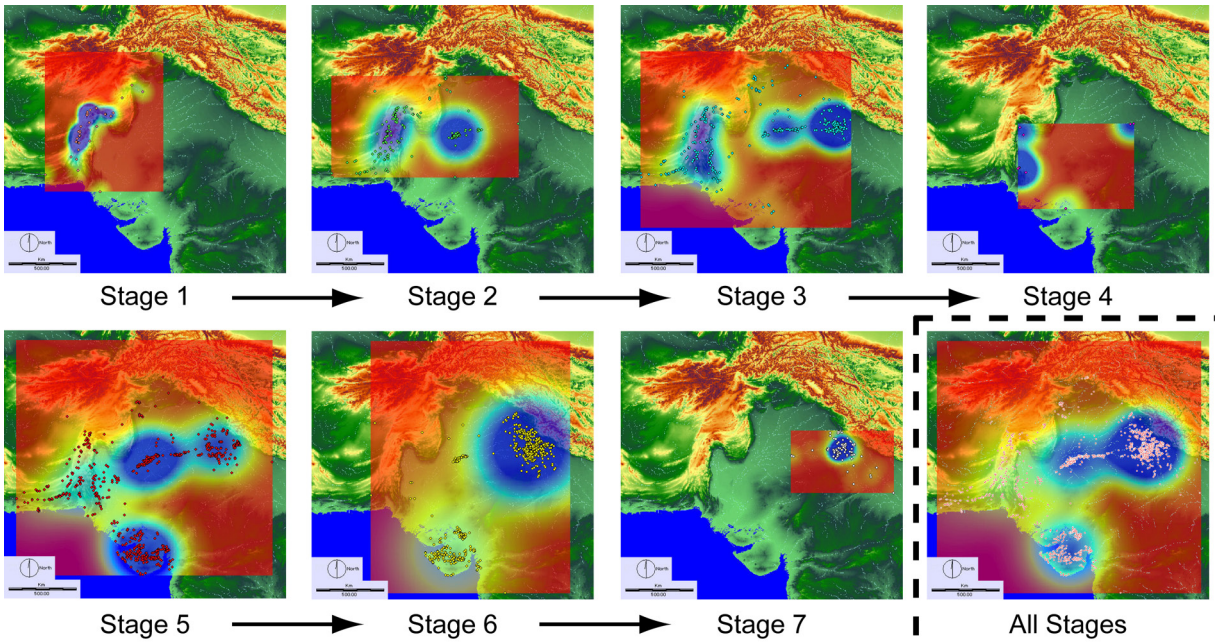

Figure 5.1.41 Diachronic changes of the site density distribution

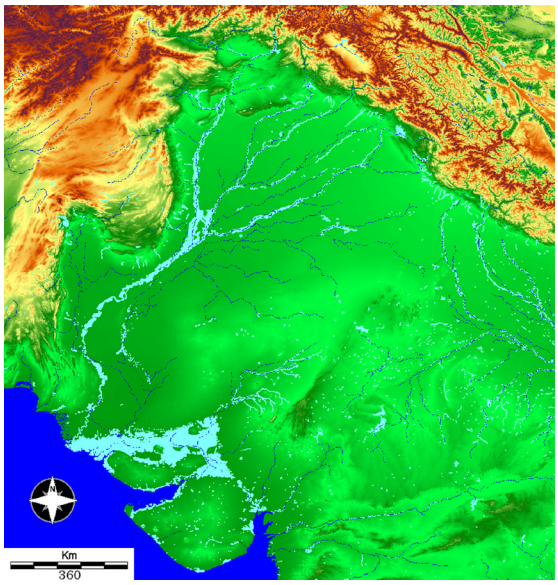

Figure 5.1.42 Run-off simulation of the Indus Valleye

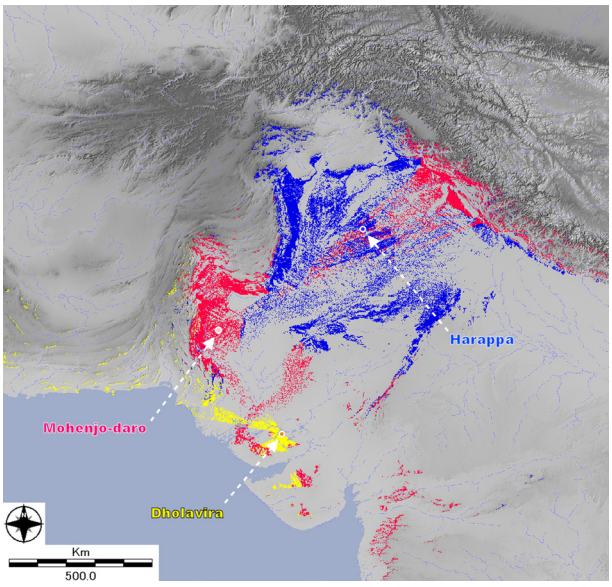

Figure 5.1.43 Visible areas from the three major Harappan sites

elevation of the Rann area is as low as the present sea level, and thus some parts of the dry land are in the same color as the sea in the SRTM-based DEM. This error is probably caused by the low resolution of SRTM. Nevertheless the analytical map is meaningful because it clearly indicates that higher places were more likely to be occupied in order to avoid floodwaters in the rainy season.

Figure 5.1.45 shows visible areas from both Dholavira and Kanmer. The former stretches from the south to southwest, while the latter covers the closed-off section of the bay from the east to southeast. These two sites are invisible for each other. However, it is noted that these two sites are located at the best places for overlooking the outlet of the bay (to the west) and the inner bay (to the east) to monitor the marine traffic. This suggests a significance of the navigation routes. In fact, the incipient phase of the Harappan Civilization corresponds to the hypsithermal period with

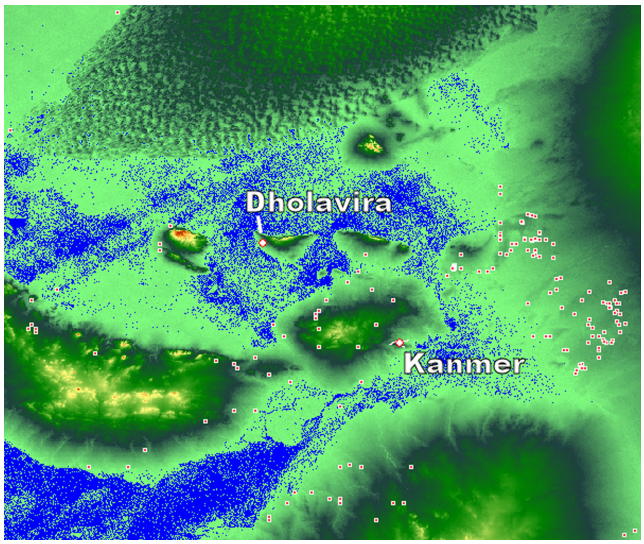

Figure 5.1.44 Archaeological sites in the Rann of Kuchchh region

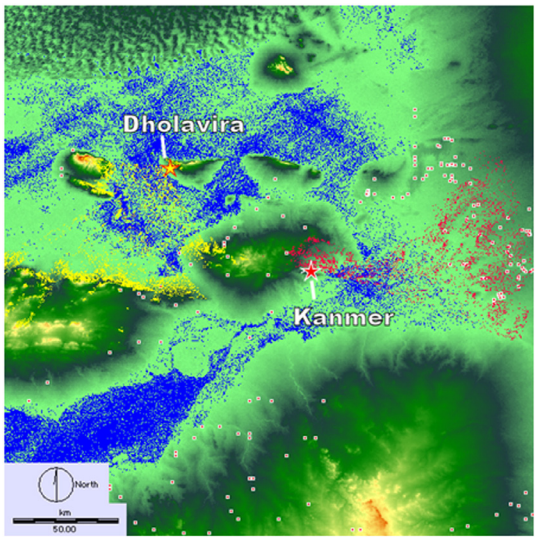

Figure 5.1.45 Visible areas from Dholavira and Kanmer

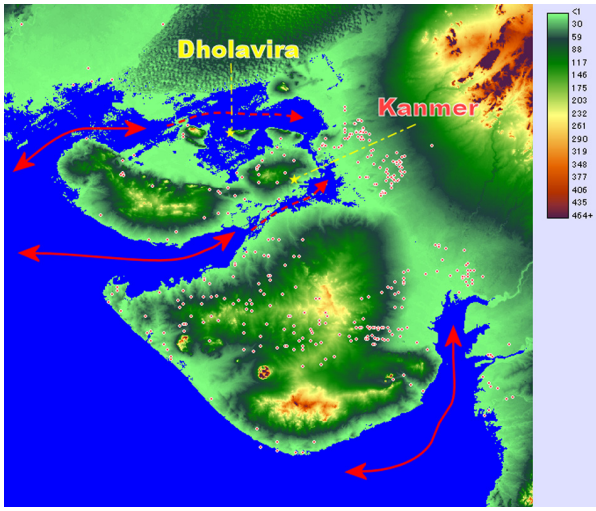

Figure 5.1.46 Sea level simulation: + 1 m ASL

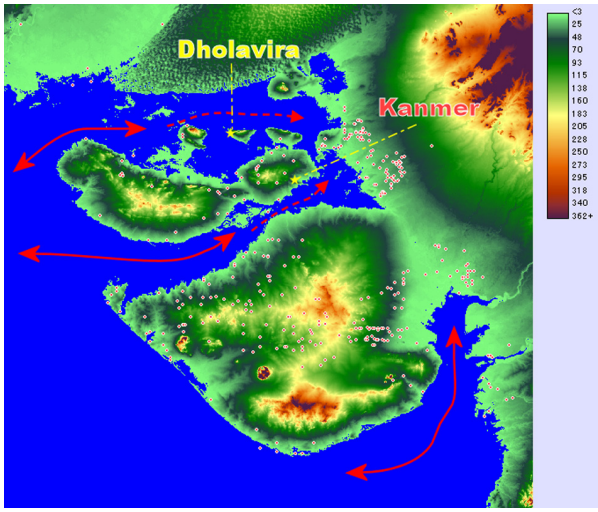

Figure 5.1.47 Sea level simulation: + 3 m ASL

marine transgression, and its collapse occurred in the cooler interval with marine regression. These notations suggest that the closure of the seaway, due to the sea level depression, might result in the declination of the Harappan sites in Gujarat and other parts of the Greater Indus region.

In order to attest this hypothesis, transformation of the seaway is simulated by different sea levels (Figures 5.1.46 and 47). A 1-m-rise of the sea level would open the seaway between the outer ocean and the closed-off section of the bay (Figure 5.1.46). Furthermore, at a 3-m-rise, seagoing crafts could reach the innermost bay of the Saurashtra peninsula where the Harappan sites were clustered (Figure 5.1.47). Direct access to the inner bay by ship would become possible at a 1.5-m-rise, whereas the strait would be closed at 1 m ASL (above sea level) and below, which would augment isolation of the inland sites. In our view, the closure of the seaway due to marine regression should be a key factor of the collapse of the Harappan Civilization. A more in-depth analysis based on a higher-precision DEM, information of the current sea level in Gujarat and the recent regional survey data will contribute to revise this view in the future.

Transformation of the Settlement Location

The above-mentioned spatial analyses of the distribution of the Harappan urban sites and local settlements have revealed the following notations concerning the diachronic change of the site location.

Stage 1: There is a dense cluster of setttlements in the Balochistan Hills in the west of the Indus Plain. Given that the Harappan Civilization originated from the eastern frontier of the Iranian Neolithic cultures (Agrawal and Kharakwal 2003), this stage would reflect the situation that the Iranian predecessors got ready to orient the natural environment of the Indus plain.

Stage 2: This stage is characterized by the foray into the Indus Plain. It is assumed that the living environment in the Indus Plain was improved by the significant increase of precipitation and average temperature during the Middle Holocene (Singh *et al*. 1973, Agrawal and Sood 1982, Bryson 1988). The increase of rainfall in both summer and winter could benefit the stable agricultural production. For instance, a convergence of archaeological sites around Harappa may result from the constant water flow of the Ravi River. It still remains to elucidate other humanistic aspects such as inception of the bund protection technology that is to flourish in the Mature Harappan period.

Stage 3: In parallel to the increase of sites in the Indus Plain, there also appeared a number of settlements in the littoral zone of northwest India, as well as in the Upper Ganges Valley. By this stage have emerged many of the typical cultural aspects of the Mature Harappan Civilization, such as fortified citadels and extensive distribution of silver, lapis lazuli and steatite ornaments. Therefore, it is conceivable that both settlement distribution and socio-cultural aspects of the Mature Harappan were developed during this period.

Stage 4: A sharp decline of settlements is observed in this stage. This phenomenon can be interpreted as a significant social change preceding the formation of the Mature Harappan Civilization. However, we should also note the relatively short time span of this stage, evidenced by the fact that some of the pottery dated to the final phase of the Early Harappan have been found together with those dated to the incipient phase of the Mature Harappan period (Agrawal and Kharakwal 2003).

Stage 5: This stage corresponds to the Mature Harappan. There are two centers in the site distribution: the Upper Indus Valley where Harappa (a type-site of this civilization) is located and the Gujarat region. Another center is observed in the Upper Ganges Valley although it is smaller than the former two. The site density in the Lower Indus and the hilly flanks in its west, where Mohenjo-daro (another type-site) is located, is relatively lower than that in the Upper Indus and Gujarat regions. The appearance of as dense a cluster of settlements in Gujarat as in the Upper Indus suggests that the trade activities connecting this region to West Asia via Oman Peninsula provided a great prosperity for the Mature Harappan community.

Stage 6: It is in this stage that the decline of the Harappan Civilization sites began. There are a number of hypotheses about the causes of this decline, but here the site distribution maps clearly shows a decrease of sites in the Mohenjo-daro area and a simultaneous increase in the Upper Ganges Valley. This indicates a shift from concentrated residence in cities to dispersed settlements and/or the population movement from

the west to the east. In addition, the sites in the Upper Indus Valley including Harappa decreased, while many sites in Gujarat continued. The social change observed here is probably derived from the deteriorating environment in the Indus Plain caused by the less rainfall as well as cooler and more arid climate, as indicated by the increase of millet cultivation and the appearance of camel, horse and donkey in the faunal assemblage. However, it is also probable that the trade activities might provide the endurance against these environmental pressures to some extent.

Stage 7: This stage is interpreted as the period when the Harappan Civilization falls into relative obscurity. The settlement cluster seems to move to the Upper Ganges Valley. The collapse of the Harappan Civilization has long been explained by the environmental deterioration or the Aryan invasion. With regard to this issue, the spatial analysis of the settlement distribution suggests that the decay of the Gujarat sites, resulted from the diminishment of port facilities associated with the sea level regression as well as the colder and drier climate, might directly affect that of the entire Harappan Civilization.

Concluding Remarks

In this paragraph, the authors have examined the rise and fall of the Harappan urban settlements by a series of GIS-aided spatial analyses, which have yielded a variety of important notations. The holistic interpretation of them lets us conclude that the transformation of the early civilization was significantly associated with the diachronic changes of the natural environment and that the trade activities played an important role in development and long-term prosperity of the civilization.

This study has dealt with the currently available temporal-spatial information on the Harappan Civilization sites. The authors are planning to obtain more data, to integrate them into GIS, and then to carry out the further research with multilateral approaches. By doing this, we will be able to clarify the significance of the Harappan Civilization in the human history.

Conclusion and Future Tasks

The archaeology-GIS team of the Indus Project has been advancing the archaeological fieldwork and research in order to publish the high-quality archaeological information about the Harappan Civilization sites as the primary goal. This chapter has reported the accomplishments of out project at the moment. Here, in the final part of the paper, the achievements are summarized and the future tasks and perspectives are overviewed.

The authors have put GIS-aided archaeology into practice at three spatial scales: (1) the supra-regional level covering the entire horizon of the Harappan Civilization; (2) the regional level focusing on the states of Gujarat, Haryana and Rajasthan in India; and (3) the site level targeting the individual settlements excavated by our project including Kanmer and Farmana.

First, at the supra-regional research level, the temporal-spatial data of more than 2,000 archaeological sites, the location and dating of which had been published, were input to the geodatabase, and then a series of site distribution maps were created from the database to be overlaid on the 1-km-grid DEM (SRTM-30). The site distribution density at each chronological phase was also analyzed to illuminate the macro-scale transformation of the Harappan Civilization. The results of this analysis indicate a dramatic increase of the settlements in the Gujarat region in the Mature Harappan period as well as a decline of the sites in Pakistan and the coincided increase

of those in the northwest part of India in the Late Harappan period. The run-off and viewshed analyses have also revealed that so-called "mega-sites" in the proximity of the large river, such as Mohenjo-Daro and Harappa, are located at the center of the great plain with a fine view, while the visibility from the major sites in Gujarat is rather restricted.

The fundamental tasks of the supra-regional spatial analysis in the near future involve refining the temporal-spatial data of the sites that have been already reported and collecting information of unknown sites in the region where the archaeological survey has not yet fully conducted. Data update in GIS is so easy that it will be very effective for these jobs. In addition, when GIS is made possible to handle more voluminous data in the future, the current 1-km-grid DEM will be replaced by higher-resolution substitutes and then it will be possible to conduct spatial analysis at the supra-regional level in the same resolution as at the current regional level.

Second, at the regional research level, a series of spatial analyses in higher resolution than at the supra-regional level have been carried out. As a result, the simulation of sea level change has inferred that the inland area surrounding Kanmer and Dholavira would sink in the navigable sea (or at least water corridor) when the sea level were 3 m higher (in geoid height) than the present days. This waterway was most likely to be present because the climate in the third millennium BCE was milder than today. Furthermore, the viewshed analysis has attested that Kanmer and Dholavira are invisible from each other and that they are located at the point from which the neighboring water zone is highly visible.

The GIS-aided spatial analysis at the regional scale has gotten increasingly popular in understanding the location and network of settlements or distribution of archaeological objects. Therefore, a refinement of the regional approaches in the near future will significantly advance these kinds of study. The fundamental tasks at this level include creating and utilizing a higher-resolution DEM such as 10-m-grid one and collecting site data in higher-resolution. It is also important for GIS-based regional studies in archaeology to conduct more empirical and interdisciplinary approaches in which, for example, the reconstructions of the paleoenvironment and paleotopography get involved. In addition, more effective methodology and procedure should be developed besides the existing methods and theories.

Third, at the target site level, the authors have been seeking to have all the archaeological finds from the site recorded as georeferenced digital data. This is a trial approach to renovate the traditional paper-based documentation. It will also potentially contribute to advance GIS-aided archaeological research.

In the excavation, the topographic survey of the target site and the surrounding areas by means of high-precision GPS and Total Station is conducted at first. Then, the acquired data are converted to the high-resolution DEM that is to be used as a base map of the excavation. The built and object remains found in situ are recorded by Total Station and photogrammetry to acquire X, Y and Z coordinate and digital imagery respectively. These data are incorporated into an othroimagery to be displayed on the base map. The soil profiles are documented in the same way. Furthermore, it has become possible to overlay the data obtained by the scientific approaches such as GPR survey on the base map and the architectural plans by means of the unified geospatial information. In addition, the archaeological objects will be ready for spatial analyses after the completion of the object databases with temporal-spatial information. In our view, these digital data are much more useful

for in-depth discussion on the size, orientation, layout and function of the site and the built structures than the conventional paper-based documents.

There are still a number of technical issues in putting such a digital-aided general research into practice. Firstly, the technique of photogrammetry, particularly preparation of a good shooting environment should be improved further. Secondly, mobile and immobile remains should be modeled in the three-dimensional format, attached with their texture, and georeferenced. This kind of approach has been put to practical use to some extent by laser-scanning technology, but there remains room for enhancing its practicality in order to replace other documentation methods. The high-quality three-dimensional scanning will achieve the highest-level documentation in archaeological fieldwork, and therefore it will contribute to advance the quality of analysis of archaeological information.

So far, the results and future tasks of GIS-aided archaeology in the Indus Project have been presented. The goal of our study in the near future is to develop the research environment in which all the archaeological work is conducted on GIS. In our perspective, this task will be achieved in multiple and seamless scales, ranging from the micro (artifact and built structure) to macro (regional) levels, when the above-mentioned issues have been solved.

Furthermore, the authors plan to apply the effective facilities of GIS not only for archaeology but also for interdisciplinary research. GIS is able to manage and analyze any kinds of information only if four essential elements of information – serial identifier, attributes, time period and geospatial location – are prepared. The next step will be the development of the “Web-GIS” in which the dataset incorporated to GIS is managed and analyzed online, taking full advantage of digital data and intelligence shared on the Internet. Taking these perspectives into account, the authors have been attempting to integrate and manage in GIS a variety of study resources of the Indus Project, including research data of linguistics, ethnology, botany and zoology other than archaeology. In our view, this trial will contribute to the establishment of Geographic Information Science, a brand-new general study discipline in the future.

2. Archaeomagnetic Study at the Kanmer, Farmana and Shikarpur Sites in India

Hideo Sakai, Yukiko Takeuchi, Takashi Ito and Takao Uno

1. Introduction

Archaeomagnetic research is generally conducted for the purpose of dating the archaeological objects, elucidating the ancient environment, and establishing other relationships by analyzing the magnetic properties of archaeological remains. In this chapter, we will present the results of archaeomagnetic research carried out at the Farmana site in Haryana state, and the Kanmer, Shikarpur sites in Gujarat state.

In India, the archaeomagnetic data from earlier studies has been inadequate, so that it is difficult to date the samples by the archaeomagnetic method. Therefore, we use archaeomagnetic direction data to examine the relative age of archaeological sites. Further, using the archaeomagnetic intensity data, we intend to examine the recent attractive hypothesis that geomagnetism has influenced the environment and paleo-climate (Gallet *et al.*, 2006).

2. Samples and outline of studied sites

Figure 5.2.1 shows the locations of studied sites.

2.1. Farmana site at Rohtak, Haryana state

This is the second-largest Harappan site in this area, considered to have prospered due to its fertile agricultural land and rich water supply. The upper layers from the mature Harappan period were removed by agricultural activity in the central area of the site, but lower layers of the mature and early Harappan periods are well preserved, and abundant artifacts of the early and mature Harappan periods have been excavated.

We collected the fired soil from the trench 3T in structural complex No.3 and from trenches 3I

Figure 5.2.1 Site locations

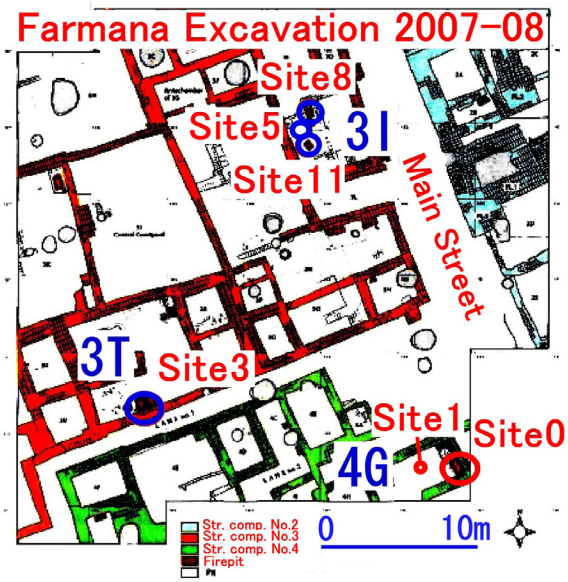

Figure 5.2.2 Farmana sampling sites, modified from the figure of Shinde *et al.* (2008)

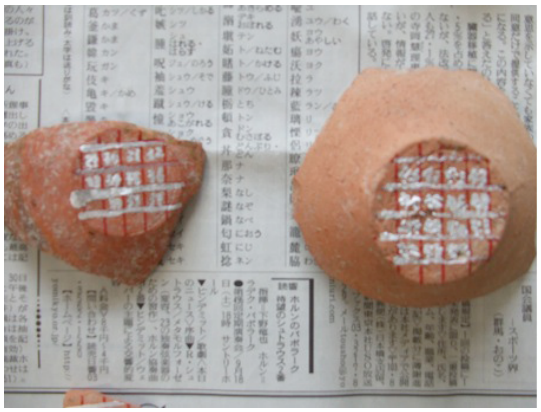

Figure 5.2.3 Examples of pottery sampled at the Kanmer site

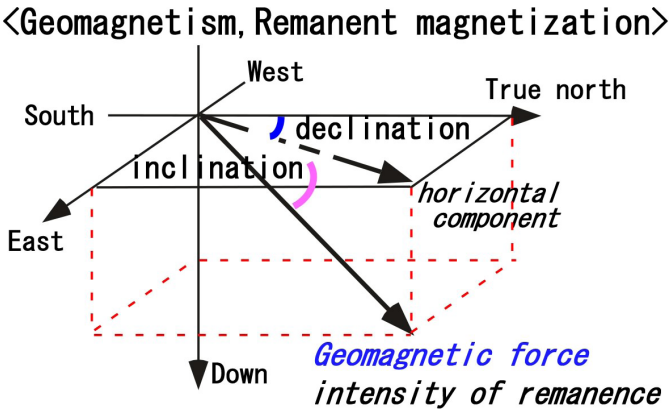

Figure 5.2.4 Geomagnetic declination, inclination and intensity (total force).
Remanent magnetization of a sample has the characteristics of declination, inclination, and intensity.

and 4G in structural complex No.4 (Figure 5.2.2). Passage soil was also sampled at trench 4G, and two bricks from surface sampling were also used in this study.

2.2. Kanmer site in Gujarat state

This is a mound-shaped citadel site composed of layers from the mature Harappan A/B and late Harappan periods. Buildings and passages of each period were excavated at a central trench, and a piled stone wall was excavated at the edge of the mound.

Fired soil of the mature Harappan-A period was sampled at Y30 of trench SE and at Z28 of trench NE, and that of the mature Harappan-B period was collected at Y28 of the central trench. Also, we used 8 sherds of pottery in the study, whose origin ranged from the mature Harappan period to the Historical period (Figure 5.2.3).

3. Remanent magnetization and geomagnetism

Fired soil and/or pottery include iron oxide (magnetite or hematite), and can be magnetized. These ferromagnetic materials can be magnetized by the geomagnetic field during a heating-cooling process under geomagnetic field, and acquiring remanent magnetizations parallel to the geomagnetic field. Therefore, we can reconstruct paleo-geomagnetism by reading the remanent magnetizations. Geomagnetism and remanent magnetization can be described by 3 components as shown in Figure 5.2.4.

3.1 Demagnetization experiments

Materials in this study have acquired the remanent magnetizations in a heating-cooling process and/or in a sedimentation process. In addition to the original magnetizations, the materials sometimes have the secondary remanent magnetizations, so a demagnetization experiment is necessary to isolate the original magnetization. In this study, we conducted demagnetization experiments with alternating fields (a.f.) and heat to remove the secondary magnetization.

Measurement of magnetizations and demagnetization experiments were performed at Toyama University using a squid magnetometer (2G-760R) and thermo/a.f. demagnetization devices. The results of demagnetization experiments were ana-

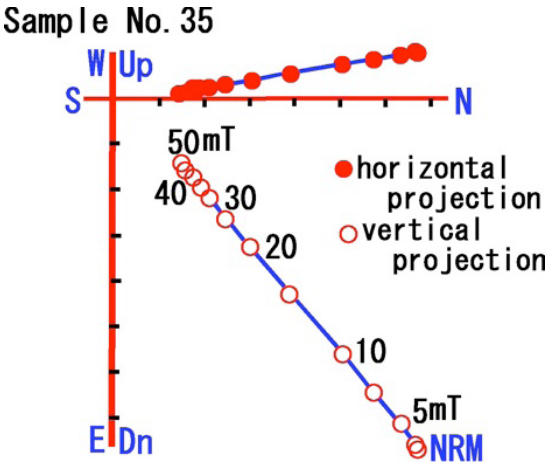

Figure 5.2.5 Progressive demagnetization result of sample No.35 shown by Zijderveld diagram.

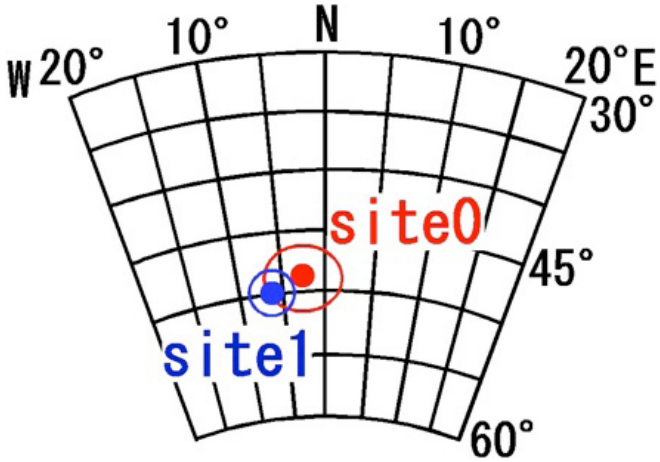

Figure 5.2.6 Schmidt net diagram of the averaged remanent magnetizations for Site 0 and Site 1 of trench 4G

Table 5.2.1 Summary of remanent magnetizations for each site

Site name	Dec.(°)	Inc.(°)	Int.(kA/m)	samples	α_{95}(°)	K
site0	−2.5	48.7	2.07E−05	4	4.5	368
site1	−6.6	50.0	3.96E−06	4	2.6	1296
site3	−7.5	43.0	1.76E−05	4	8.8	110
site5	−0.2	39.6	4.92E−05	4	2.2	1396
site8	−1.1	38.1	2.15E−05	4	2.5	428
site11	−8.7	42.3	8.13E−06	4	5.3	296

Dec, Inc.: average of declination and inclination
Int.:average intensity of remanent magnetization
samples:number of measured samles
α_{95} and K:statistical parameter of magnetic direction

lyzed in a Zijderveld diagram (Zijderveld, 1967). An example of the diagram is shown in Figure 5. This diagram is used to resolve the magnetization vector into horizontal and vertical components, and analyzes the direction and intensity of the vector on those planes. From the changes of magnetization with demagnetization in a Zijderveld diagram, a reliable remanent magnetization is obtained through the principal component analysis (Kirshvink, 1980).

For the Thellier's method of studying the archaeomagnetic intensity, please refer to Sakai and Hirooka (1986).

4. Study of remanent magnetizations and the dating at the Farmana site

Most of the samples from the Farmana site are fired soil. Figure 5.2.5 shows the Zijderveld diagram for the demagnetization of sample No.35. The demagnetization experiment was conducted in a magnetic field of 2.5 - 50 mT (milli-Tesla, unit of magnetic field). Changes of magnetic vector with demagnetization lie almost on a straight line, indicating that the original magnetism is well preserved and secondary magnetism is small.

After obtaining the stable magnetization through demagnetization experiments, we determined the

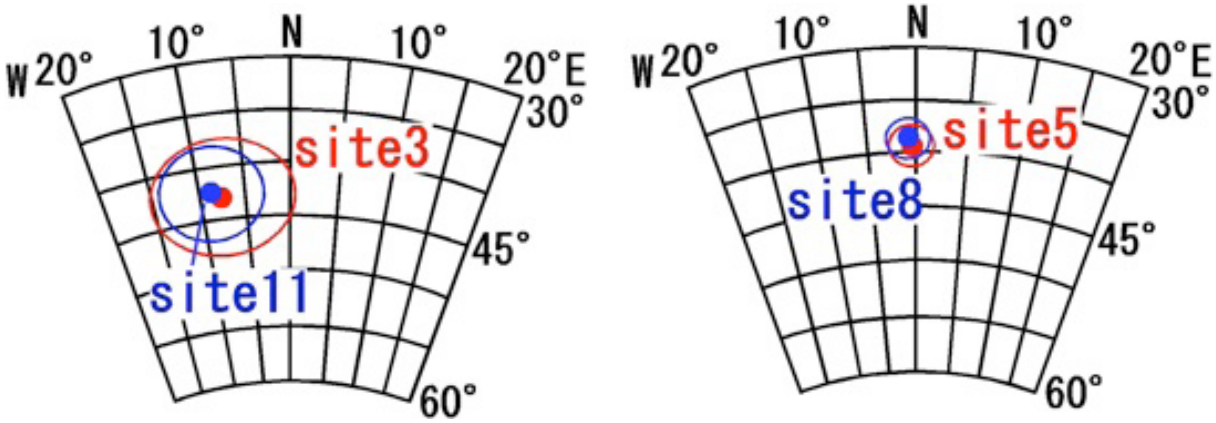

Figure 5.2.7 Schmidt net diagram of the remanent magnetizations for Sites 3, 5, 8, 11.

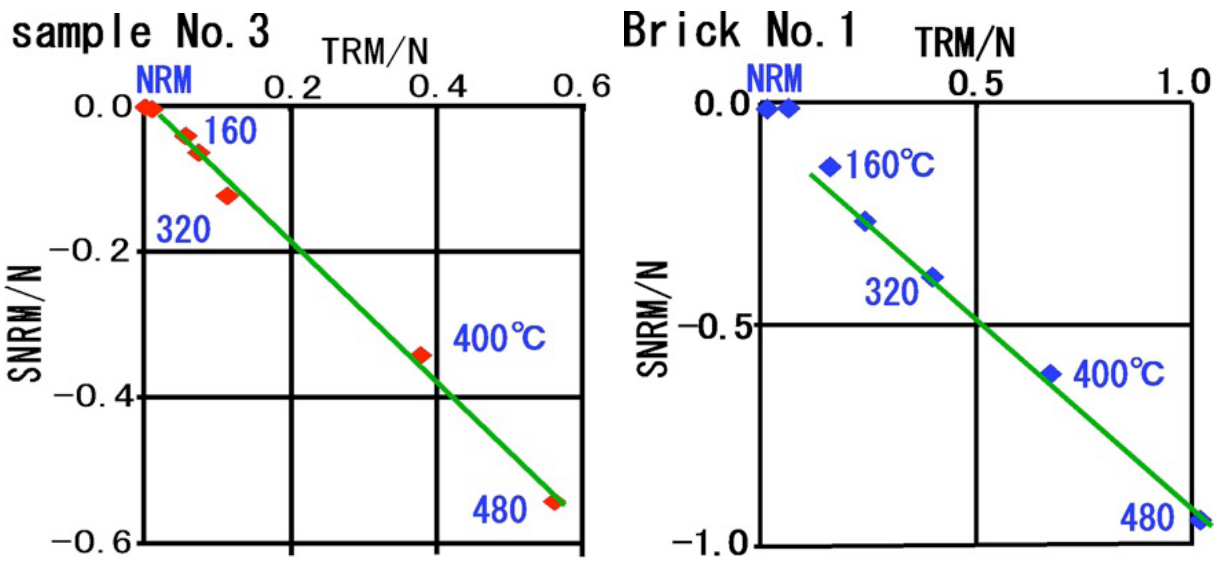

Figure 5.2.8 Typical results of Thellier's experiments shown by SNRM-TRM diagram

average direction of magnetization for each site. As a magnetic compass was used at the sampling to mark geomagnetic north on the sample, we corrected the declination data by the 0.9 degree that is the local current geomagnetic declination. Table 5.2.1 shows, magnetizations as the sites. α95 is a statistical parameter indicating the concentration of the magnetic directions, i.e. the circle of 95% confidence about the mean direction. For most of the sites, α95 angle is a few degrees, that is, the remanent magnetizations are well concentrated. Figures 5.2.6 and 5.2.7 represent the direction distribution of remanent magnetization at each site on a Schmidt net diagram.

4.1. Remanent magnetizations of the passage soil

In trench 4G, the passage soil at Site 1 and the fired soil at site 0 were studied. The remanent magnetization at Site 1 has the intensity about one fifth of that at Site 0 (Table 5.2.1), which verifies that the passage soil of Site 1 was not fired.

The magnetic directions of the two sites, as shown in the Schmidt net diagram (Figure 5.2.6), are consistent within the statistical error. This indicates that the passage soil at Site 1, having been firmly compacted by foot traffic, acquired remanent magnetizations at a similar period as the soil of Site 0. Thus, walked-on soil could be a useful material for archaeomagnetic studies.

Table 5.2.2 Summary of the results of Thellier's experiments

sample No.	age(year)	remains	NRM (kA/m)	plots number	geomagnetic intensity(μT)	R^2	range of temperature(℃)
<sherd>							
1	BC2600～1900(Mature Harappa A)	Kanmer	2.09E-03	4	38.4±0.9	0.99	160～480
2	BC2600～1900(Mature Harappa A)	Kanmer	3.54E-05	6	40.6±5.0	0.95	80～480
3	BC2600～1900(Mature Harappa B)	Kanmer	7.81E-04	6	31.7±0.1	0.99	80～480
4	BC2600～1900(Mature Harappa B)	Kanmer	5.25E-04	4	26.0±2.6	0.99	240～480
5	BC2600～1900(Mature Harappa B)	Kanmer	2.55E-03	6	30.1±1.3	0.99	80～480
6	BC1800～1000(Late Harappa)	Kanmer	1.94E-04	5	39.5±3.8	0.96	80～400
7	BC1800～1000(Late Harappa)	Kanmer	4.50E-04	5	38.3±5.4	0.97	160～480
8	BC1000～ (Roman period)	Kanmer	4.37E-03	4	54.2±4.3	0.97	80～320
<brick>							
1	about BC2500	Farmana	6.12E-03	5	29.3±1.8	0.99	240～480
2	about BC2500	Farmana	2.45E-03	5	28.0±2.1	0.98	160～480

NRM:intensity of remanent magnetization before demagnetization experiment
plots number: plots used for the estimate of geomagnetic intensity in SNRM-TRM diagram
geomagnetic intensity:estimated geomagnetic intensity
R: correlation coefficient of the pots in SNRM-TRM diagram
range of temperature:temperature range of the data used

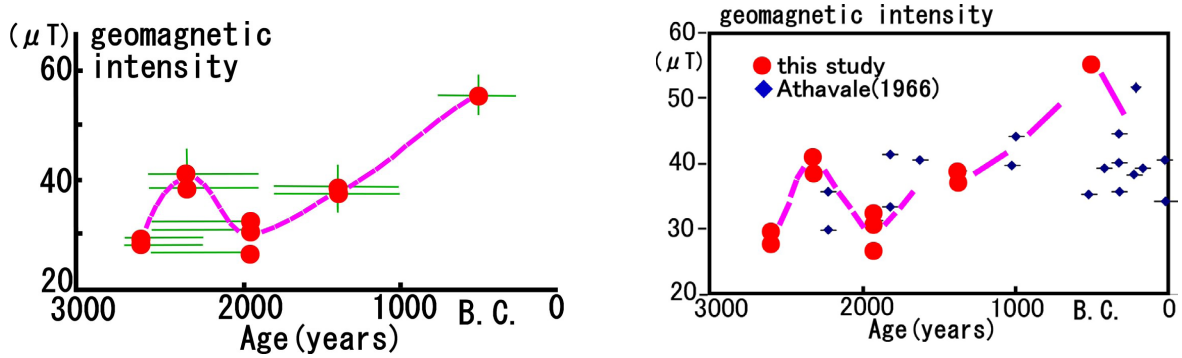

Figure 5.2.9 a (left): secular variation of the geomagnetic field intensity in India from this study
b (right): comparison of the data of this study with those by Athavale (1966)

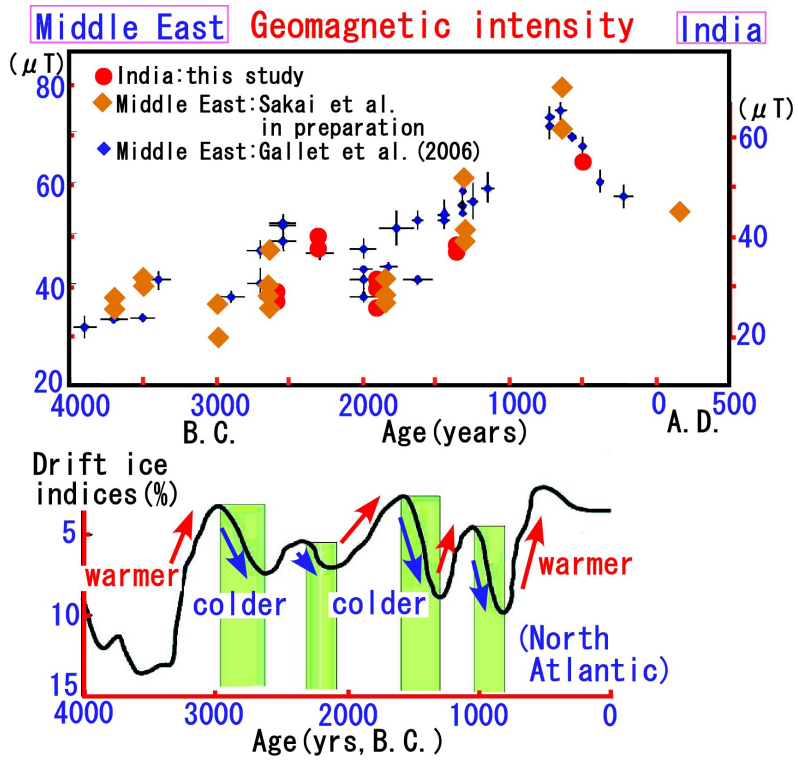

Figure 5.2.10 Upper figure shows the secular variation of geomagnetic field intensity from B.C. 4,000 to A.D. 0 in Middle Eastand India (this study).

The lower figure shows historical temperatures, estimated from drift ice indices in the North Atlantic, based on Gallet *et al.* (2006)

4.2. Classification of the studied sites by remanent magnetization

In structural complex No.3, we studied the fire pits at Site 3 of trench 3T, and those of Sites 5, 8, 11 at trench 3I. The averaged directions of remanent magnetization for these sites in Figure 5.2.7 demonstrate that the directions of Site 3 and Site 11 are similar, while those of Site 5 and Site 8 are similar.

By comparison of magnetic vectors, the investigated six sites fall into three groups: Sites 0 and 1, Sites 3 and 11, Sites 5 and 8. This might correspond to the sites having different ages, so it is expected that this classification will be examined by archaeological chronology in the future.

5. Variation of geomagnetic field intensity elucidated from Thellier's method

Thellier's experiment was conducted on the sherds and bricks. Heating of the samples was performed in 80℃ steps from 80 to 480℃ . In Figure 5.2.8, the results of experiment for sherd No.3 and brick No.1 (Table 5.2.2) are shown in SNRM-TRM diagrams.

Similary to Figure 5.2.8, the results of Thellier's experiment for many samples produce an SNRM-TRM diagram in which the data lie on a straight line. For these samples, the historical geomagnetic intensity was successfully estimated from the straight line. The data obtained are summarized in Table 5.2.2.

Figure 5.2.9a represents the time variation of geomagnetic intensity elucidated in this study. For India, Athavale (1966) published the archaeomagnetic intensities (Figure 5.2.9b). The data are so old that it is difficult to examine their reliabiity, but they consistent with our data, the variation of geomagnetic intensity from 3,000 years BC to 0 AD is almost concordant. Further studies are expected in order to create a standard variation of geomagnetic intensity, which may be useful for dating archaeological objects in India.

5.1. Comparison of geomagnetic field intensity variation between India and Middle East

The upper diagram in Figure 5.2.10 summarizes the geomagnetic intensities in the Middle East and those in India in this study. Data for the Middle East are from studies by Gallet *et al*. (2006) and Sakai *et al*. (in preparation). The right-hand scale of the vertical axis (geomagnetic intensity) has been adjusted slightly for India because of the difference of geomagnetic intensity due to the latitude difference of the two areas. There are common characteristics between the variation of the geomagnetic field intensity in India and that in the Middle East.

The lower graph in Figure 5.2.10 shows the temperature variation estimated from the drift of ice indices in the North Atlantic area (Gallet *et al*., 2006), with the scale of the vertical axis inverted from the original figure.

Gallet *et al*. (2006) proposed that the geomagnetic field intensity changed suddenly around 3,000 years BC, which matches the climatic change. Further, they maintain that the sudden change in secular variation of the geomagnetic field intensity caused climatic change and influenced the course of civilization. From Figure 5.2.10, where our data are combined, the idea of Gallet *et al*. (2006) seems to have merit. There is a possible relation between the geomagnetic field intensity and the climate.

Changes in geomagnetic intensity reflect activity in Earth's core. They influence the global environment by the interaction between the geomagnetic (extraterrestrial) field and the solar wind, so the study of magnetic intensity variations from

prehistory to the present is important. If changes in geomagnetism and climate or global changes in the environment are related to changes in the early Indus civilization, this is an important subject that requires further serious study.

3. Ground Penetrating Survey at Kanmer Site, India

Toru Kishida, Asuka Kanto and Hideo Sakai

GPR Survey in 2007 - 2008 season: Inside of the Citadel mound

1. Forward

Kanmer is a citadel site of the Harappan period. The excavations at the site have recovered some parts of the massive wall with dual (outer and inner) stone surfaces. The nondestructive GPR survey was carried out on these walls in order to predict the position of the unburied wall and gate structures.

2. Outlines of GPR survey

GPR (ground penetrating radar) survey is a method to detect underground structures by physical response such as reflection, inflection, penetration and attenuation of electromagnetic (radar) wave. A pair of antennae - sender and receiver - are attached to the survey instrument. Of the electromagnetic waves that had emanated from the sending antenna to penetrate into the underground, those that had been reflected by the discontinuous plane (or boundary plane of different electric permittivity) and then have returned to the ground surface are captured by the receiving antenna. Here, the collapsed time between the send and the reception of the electromagnetic wave (t: propagation time) and the resistivity of the reflected wave are recorded, and then a virtual GPR profile is created by placing these records in the chronological order. Electromagnetically discontinuous plane is typified by geological one (bedding plane, fault plane and boundary plane between different rocks), cavity and buried object (gas pipe for instance). When these discontinuous planes are bidimensional, the reflected figure will appear as a line, or a section of the plane structure, in the GPR profile.

In GPR survey, the limit of exploring depth depends on periodicity of the antenna. In general, the periodicity in use ranges from 10 MHz to several GHz, corresponding to the high frequency (HF) to ultrahigh frequency wave (UHF) bands. Electromagnetic wave of lower frequency tends to penetrate in more depth, while that of higher frequency goes less. The resolution of the resultant data in lower frequency is coarser than that in higher frequency. Therefore, it is necessary to select an appropriate frequency (or antenna) in accordance with the depth and size of architectural or object remains on target.

The results of GPR survey often contain many noisy signals such as the reflected waves derived from the discontinuity between the antenna and the ground surface, noisy wave called as “clutter” and multipath reflected wave. These noises may result in chaotic patterns in the profile, and therefore they should be removed by a variety of the signal processing technologies to extract the wave that is correctly reflected by the target.

3. Results of survey

At the analytical phase, the three-dimensional analysis with time slice mapping (Conyers and Goodman 1997) was also applied. This analytical method integrates the GPR profiles of each traverse line and then sorts out the data with substantial running time (depth range) to draw the

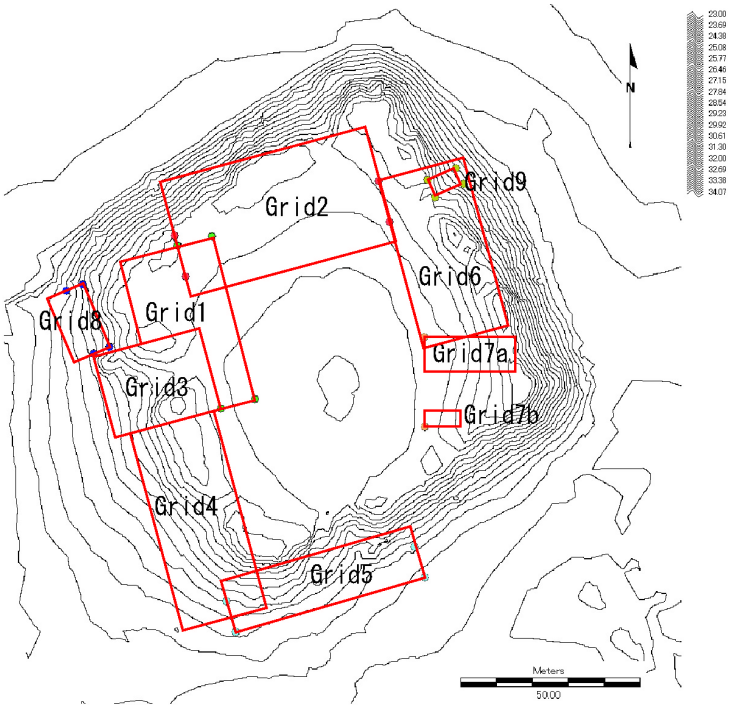

Figure 5.3.1 Areas of the GPR survey (2007 - 2008 season)

Figure 5.3.2 Snapshot of the GPR survey (2007 - 2008 season)

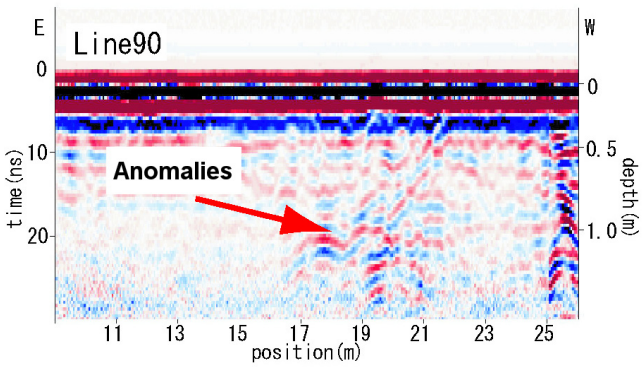

Figure 5.3.3 Representative GPR profile in Grid 1 (Line 90)

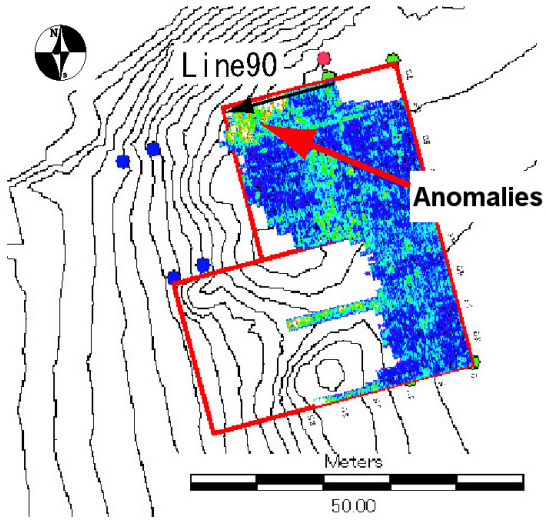

Figure 5.3.4 Time slice map of Grid 1 (Depth of analysis: 21 - 24 ns, ca. 105 - 120 cm)

underground structure within the configured depth range by means of averaging and interpolation of the relative resistivity of the reflected radar waves. As a result of the three-dimensional analysis, a number of plans in different exploring depths are drawn with different colors corresponding to different resistivity in order to examine the transformation of the abnormal response. The time slice mapping is particularly effective for the studies in which planar distribution of the exploring targets is essential. During the GPR survey, it is possible to monitor the measured data as a quasi-profile of the underground structures in real time. In addition, this method makes possible a rapid survey in high resolution. Thanks to these advantages, GPR is employed for various purposes in the field such as environmental and archaeological studies.

The GPR survey was carried out at Kanmer on 23 - 26 February 2008 (for 4 days in total). The survey employed Noggin plus 250 and the SmartCart system supplied by Sensors & Software Inc. (Canada) with 250 MHz center frequency antennae.

Figure 5.3.1 presents the areas of survey, namely Grids 1 to 9, located in the upper periphery of the citadel. The traverse lines were laid out in every 0.5 m in Grids 1, 2, 3 and 7 and every 1 m in Grids 4, 5, 6, 8 and 9. In total, 468 traverse lines were surveyed. Figure 5.3.2 is a snapshot of the survey. It was rather hard to push the survey cart because most of the areas were slope and numerous obstructing stones were scattered on the ground surface. Thus in the upslope session, the cart was dragged up with the rope fastened to its front. The results of survey are described in the following.

GRID 1: Figure 5.3.3 shows the GPR profile acquired on a typical traverse (Line 90). An abnormal response occurred in the position (distance from the start point of the traverse line) between 17 and 20 m and ca. 1 m in depth. The aberration was concentrated in the northwest corner of the grid. There is no remarkable abnormal response in the rest of the grid. The existence of inner wall had been predicted according to the results of the previous excavations, but no trace was acquired by the GPR survey. The inner wall would be buried over 1.5 m deep. Figure 5.3.4 is a time slice map analyzing the underground between 105 and 120 cm in depth from the ground surface. It indicates that the abnormal response in the northwest corner of the grid, as appeared in Figure 5.3.3, stretches even outside of the grid. Although the strength of response is unclear, it suggests a possibility of the presence of some architectural remains.

GRID 2: Figure 5.3.5 presents the GPR profile of a typical traverse (Line 48). In this grid, there is no abnormal response that could be clearly interpreted as mural remains. The inner wall was recovered in the trench located in the northeast part of the grid, but the GPR survey could not detect any traces of it. The inner wall appears to be buried too deeply to be distinguished by the survey instrument. Figure 5.3.6 shows a time slice map of Grid 2, analyzing the underground between 105 and 120 cm in depth, where some abnormal responses were captured. However, those do not appear to correspond to any built structures.

GRID 3: Figure 5.3.7 is the GPR profile of a typical traverse (Line 0). Strong abnormal responses were observed in the position between 12 and 20 m as well as between 22 and 24 m and in the depth between 0.5 and 1.7 m. The response in the position between 22 and 24 m probably indicates the outer wall of the citadel. Another structure, possibly a large building, is predicted

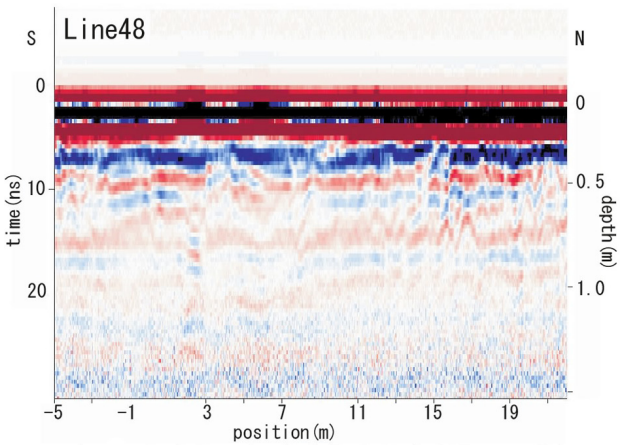

Figure 5.3.5 Representative GPR profile in Grid 2 (Line 48)

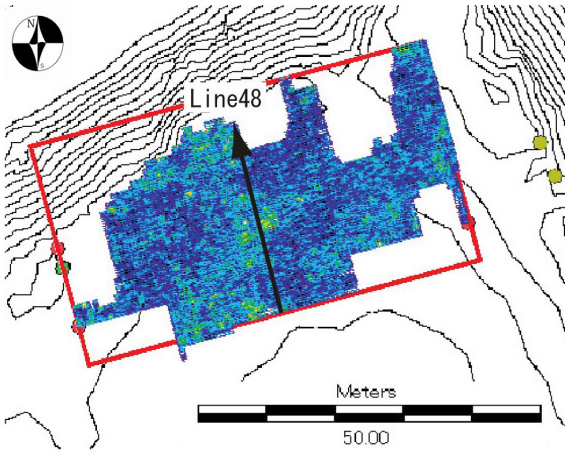

Figure 5.3.6 Time slice map of Grid 2 (Depth of analysis: 21 - 24 ns, ca. 105 - 120 cm)

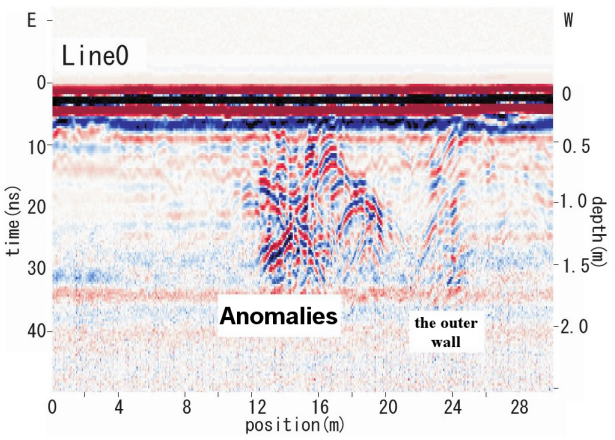

Figure 5.3.7 Representative GPR profile in Grid 3 (Line 0)

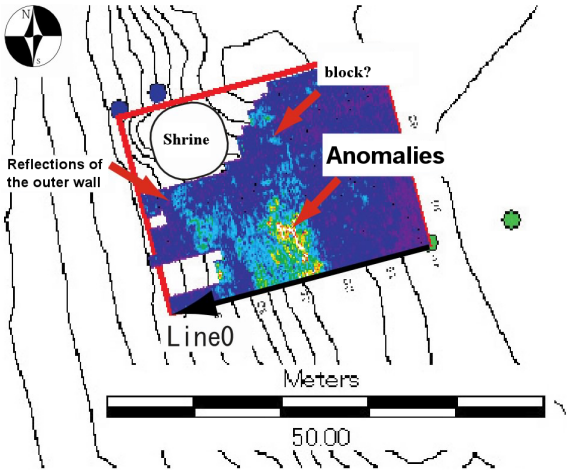

Figure 5.3.8 Time slice map of Grid 3 (Depth of analysis: 20 - 25 ns, ca. 100 - 125 cm)

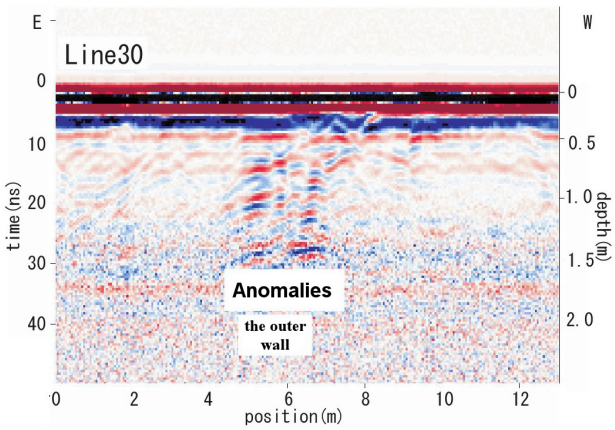

Figure 5.3.9 Representative GPR profile in Grid 4 (Line 30)

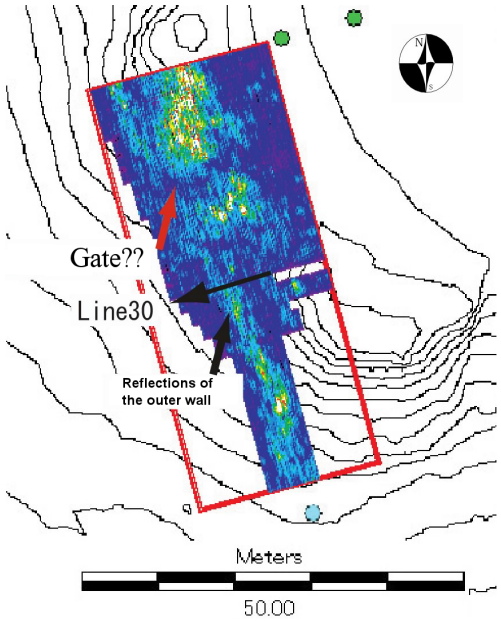

Figure 5.3.10 Time slice map of Grid 4 (Depth of analysis: 20 - 25 ns, ca. 100 - 125 cm)

by the abnormal response in 8 m wide inside the outer wall. In Figure 3-65, a time slice pattern of the underground between 100 and 125 cm in depth is displayed. The abnormal response observed in the western end of this grid can be interpreted as a trace of the outer wall stretching straightforward from the north to the south. The response observed in the position between 12 and 20 m (Figure 5.3.8) is running in parallel to the outer wall and clearly ends up at the point just a little east of the central zone of the grid. At the northern side of that point, there is another abnormal response in a circular shape. It is assumed to be an effect of topography because this part is correspondent to a large pocket of the ground surface.

GRID 4: Figure 5.3.9 shows the GPR profile acquired on a typical traverse (Line 30). There is a zone of relatively strong abnormal response in the position between 5 and 7 m and in the depth between 0.5 and 1.7 m. This abnormality is probably a continuous trace of the outer wall observed in Grid 3. Figure 5.3.10 presents a time slice map analyzing the underground between 100 and 125 cm in depth. This map clearly indicates the outer wall running straightforward from the north to the south. However, the wall is discontinuous at the point just a little north of the central zone of this grid (indicated by a red arrow in Figure 5.3.10). The discontinuous zone is 5 m wide, and it is possibly a gate of the citadel.

GRID 5: The GPR profile of a typical traverse (Line 20) is shown in Figure 5.3.11. A zone of abnormal response is observed in the position between 14 and 16 m and in the depth between 0 and 1.5 m. This aberrance probably indicates the outer wall of the southern side of the citadel. The time slice map analyzing the unburied structures between ca. 100 and 125 cm in depth (Figure 5.3.12) clearly distinguishes a trace of the outer wall that stretches in the western side of the citadel from the north to the south. It appears to turn off to the east at the southwest corner of the grid. This may correspond to the southwest corner of the outer wall. The outer wall is then running straightforward to the northeast, continuing to the outside of the grid. There is no discontinuity in the outer wall line that would indicate the location of a citadel gate. In addition, the linear abnormal response running in the eastern part of the grid from the northwest to the southeast is an effect of surface water from the higher zone of the citadel and thus it does not reflect the actual situation of the underground.

GRID 6: The GPR profile of a typical traverse (Line 10) shows a zone of abnormal response in the position between 14 and 16 m and in the depth between 0 and 1.5 m (Figure 5.3.13). The similar abnormality is also observed on another traverse located at 1 m south of Line 10. Figure 5.3.14 presents a time slice map analyzing the underground between 100 and 125 cm in depth. The aberrance captured on Line 10 appears to extend to the east of Grid 6, but the limit and size are blurred. There is no abnormal response that indicates any other architectural remains.

GRID 7: Figure 5.3.15 is the GPR profile of a typical traverse (Line 15) that indicates no remarkable abnormal response. The time slice map analyzing the underground between ca. 50 and 75 cm in depth (Figure 5.3.16) shows a cluster of relatively small responses. This grid was set in the neighborhood of the trench from which the remains of a building were recovered beneath the ground surface (1m or less in depth). However, the GPR survey could not distinguish any traces of it because it was very difficult to scan the wall in the circumstance that many of wall stones collapsed and scattered.

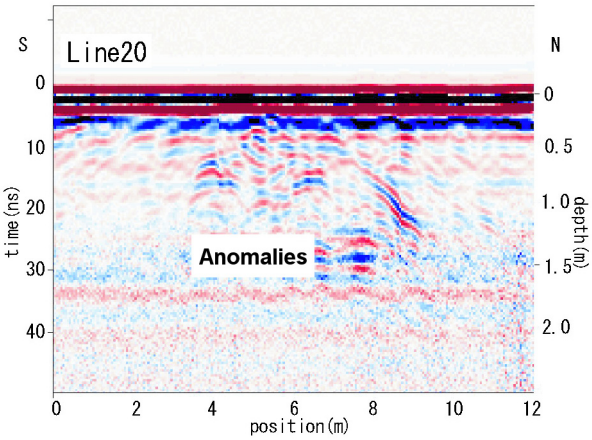

Figure 5.3.11 Representative GPR profile in Grid 5 (Line 20)

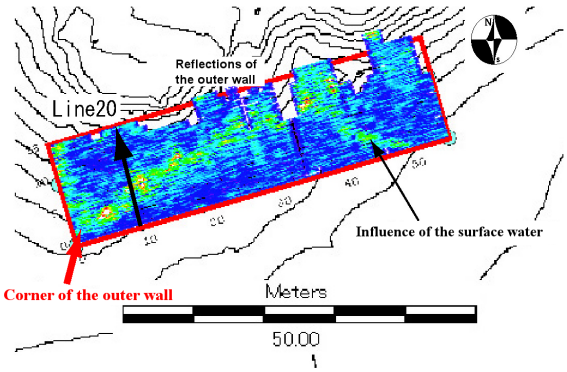

Figure 5.3.12 Time slice map of Grid 5 (Depth of analysis: 20 - 25 ns, ca. 100 - 125 cm)

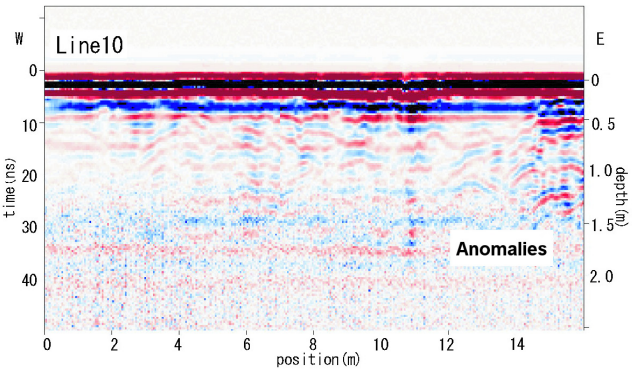

Figure 5.3.13 Representative GPR profile in Grid 6 (Line 10)

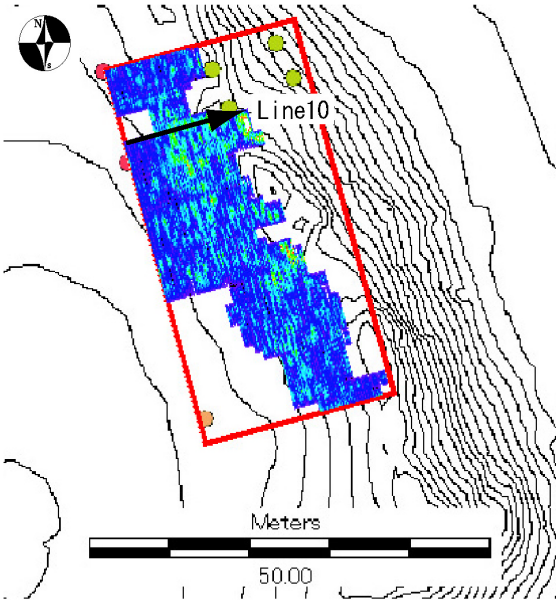

Figure 5.3.14 Time slice map of Grid 6 (Depth of analysis: 20 - 25 ns, ca. 100 - 125 cm)

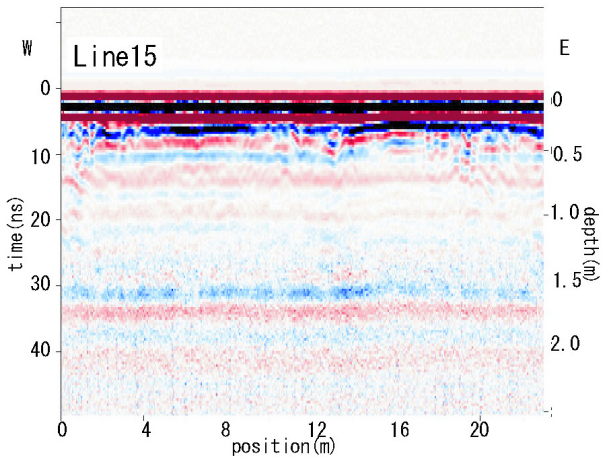

Figure 5.3.15 Representative GPR profile in Grid 7 (Line 15)

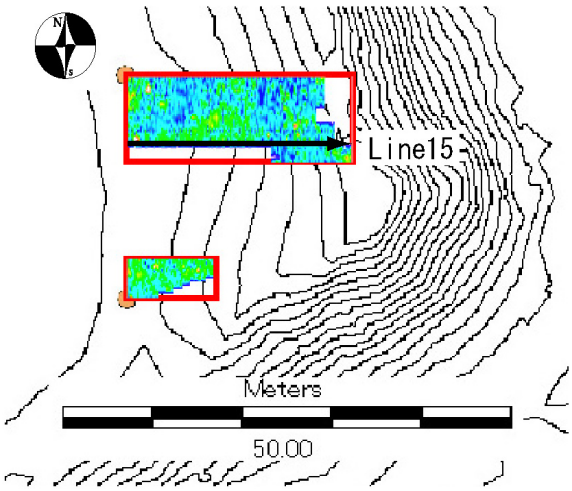

Figure 5.3.16 Time slice map of Grid 7 (Depth of analysis: 10 - 15 ns, ca. 50 - 75 cm)

GRID 8: The GPR profile of a typical traverse (Line 10) shows a strong abnormal response in the position between 0 and 4m and in the depth between 1 and 1.7m (Figure 5.3.17). This abnormality is associated with the outer wall in the western side of the citadel. The width of the strong response is more than 4m. This may reflect collapse and scatter of the wall stones. The time slice map analyzing the unburied structures between ca. 75 and 100cm in depth (Figure 5.3.18) indicates a trace of the outer wall running from the northwest to southeast. The northwest corner of the outer wall was recovered in the previous season, and therefore, the outer wall detected in this grid probably connects to that.

GRID 9: Figure 5.3.19 is the GPR profile acquired on a typical traverse (Line 3), which indicates abnormal response in the position between 2 and 5 m and in the depth between 0.7 and 1.5m. This aberrance is associated with the outer wall in the eastern side of the citadel. Figure 5.3.20 shows a time slice map analyzing the underground between ca. 100 and 125cm in depth. It is rather difficult to determine the direction of wall because of a narrow grid (5m from the north to the south by 8m from the east to the west).

The time slice maps of all the grids are integrated with the contour of the citadel (Figure 5.3.21). In the integrated map, the outer wall is indicated by red line (the dashed parts are a prediction based on the results of the GPR survey). This map reveals that the outer wall of the eastern side orients 26.5° from the north axis to the west, whereas that of the southern side orients 57.6° from the north axis to the east. This means that the eastern wall bisect the southern one at little a bit acute angle rather than right angle. The topological map also indicates that the citadel is not a square but a quadrangle with a longer diagonal line running from the north to the south. Therefore, it is assumed that the plan of the citadel wall also looks like a parallerogram.

4. Conclusion

In summary, the GPR survey at Kanmer targeting the mural remains surrounding the citadel has revealed traces of the western wall, the western half of the southern wall, the southwest corner and part of the eastern wall. It has also suggested that the outer wall turns off at acute angle rather than right angle at the southwest corner. Furthermore, there are a few zones of strong abnormal response in the western side of the citadel (Grids 3 and 4), which are assumed as built remains. With regard to the gate, a main concern of this research, a discontinuity of the outer wall is observed in Grid 4, and thus the authors predict an entrance complex there.

All of the mural remains detected by this study belong to the outer wall. The excavations at the site had revealed that there was also an inner wall inside the outer wall, but it was invisible through the GPR survey because it was buried too deeply to be captured by the frequency of antennae used in this season as a preliminary research. The authors plan to employ other antennae to explore deeper as well as other exploring methods in order to advance the nondestructive surveys at Kanmer.

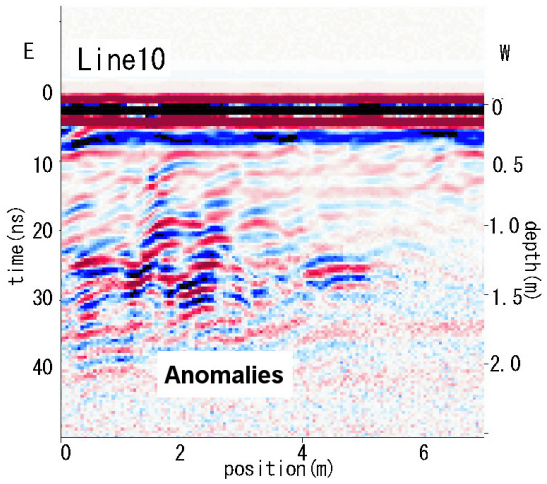

Figure 5.3.17 Representative GPR profile in Grid 8 (Line 10)

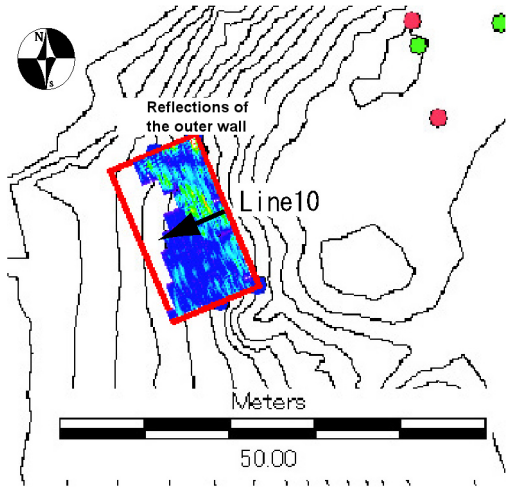

Figure 5.3.18 Time slice map of Grid 8 (Depth of analysis: 10 - 15 ns, ca. 50 - 75 cm)

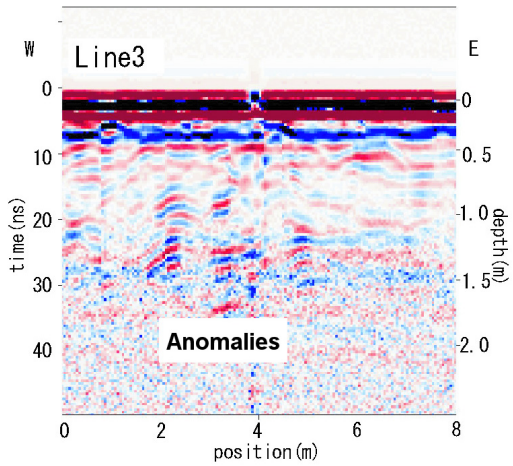

Figure 5.3.19 Representative GPR profile in Grid 9 (Line 3)

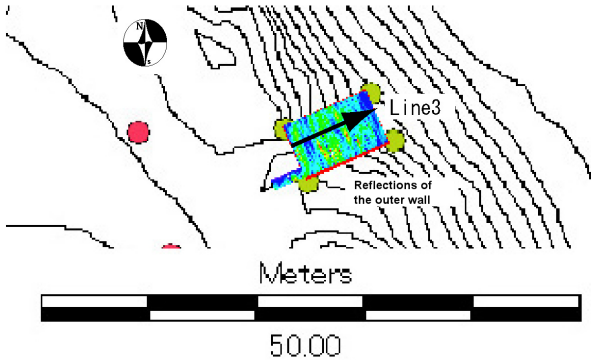

Figure 5.3.20 Time slice map of Grid 9 (Depth of analysis: 20 - 25 ns, ca. 100 - 125 cm)

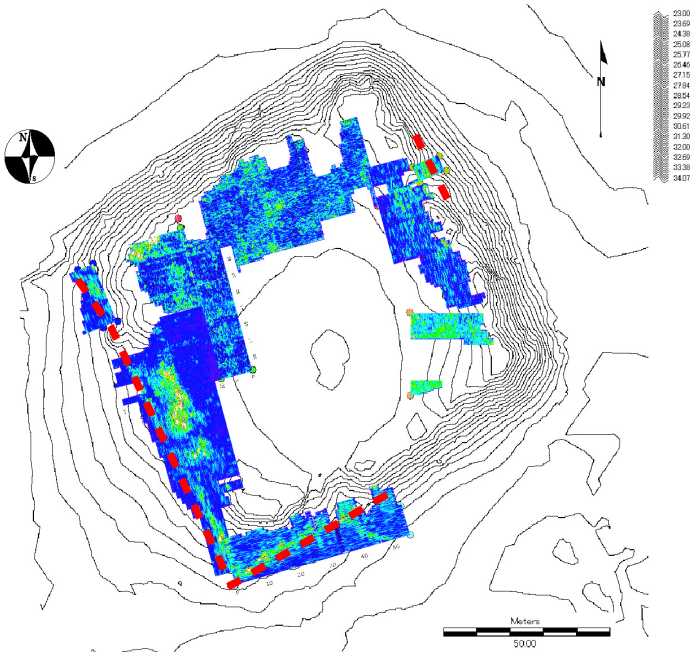

Figure 5.3.21 Location of the outer wall predicted by the results of the GPR survey

GPR Survey in 2008 - 2009 season: Outside of the Citadel mound

1. Introduction and outline of survey

We have carried out the Ground Penetrating Radar (GPR) survey at Kanmer site since 2007. In 2007, we have surveyed at upper flat and slope surface of Citadel mound, where wall of the Citadel mound with outer and inner stone piles was partly excavated. We detected straight anomalies of outer stone pile at the halfway up a slope surface, however it was difficult to detect inner stone pile which estimated to exist at about 5 meters depth from surface (Teramura *et al*. 2008).

In this chapter, we show the results of GPR survey conducted at outside of the Citadel mound in February 2009. The purpose is to detect walls or residences where facilities are estimated.

We located 6 survey areas (Grid1-6) at northern and eastern region of the Citadel mound. GPR survey was done along 0.5m interval survey lines, whose direction was west-east in Grid 1-3 and south-north in Grid 4-6 (Figure 5.3.22, 23). In these survey areas, rectangular Grid was planned using Total Station System, however as we surveyed to the edge of the Citadel mound within the limits of the possible, the survey area was distorted from rectangular shapes practically. Noggin plus (Sensors & Software Inc.) of Univ. Toyama was used as the GPR apparatus.

The survey data was analyzed mainly by GPR profile of each survey line, where the software 'EKKO View and EKKO View Deluxe' (Sensors & Software Inc.) was utilized. After getting the GPR profiles from all survey lines, time-slice map analysis was done to know the anomalies at several depths, by the software 'EKKO Mapper and Transform' (Fortner Software Inc).

In the analysis of data, determination of depth to the target is important. We took the following procedure to obtain the depth distribution. Firstly, the relative permittivity of soils is gained by applying the hyperbolic matching method (Cassidy, 2009) to the hyperbola pattern in GPR profile. Through the analysis, the average of relative permittivity of soils is determined as 0.135m/ns. Then, travel time of radar wave is obtained using this permittivity, and the depth to the target is determined.

2. Results of GPR survey

2.1. Analysis by GPR profile

Representative GPR profiles in each Grid (figure 5.3.23) are shown in the following.

GRID 1: The GPR profile of survey line 0 (top of figure 5.3.24) shows that there is an anomaly at 1-2m from the starting point. The depth of anomaly is 0.4m. Characteristics of the anomaly and strength of reflection suggest that the anomaly may be stone objects. We estimate the structure such as stone piled wall survived there.

The GPR profile of line 40 (20m north from line 0) in the bottom of Figure 5.3.24 shows a clear anomaly at 4-6m. This strong reflection composed of multiple reflections is similar to the anomaly on line 0. Therefore, we estimate that a same kind of structure remains with that at line 0.

GRID 2: The GPR profile (top of figure 5.3.25) of line 0 shows an anomaly at 11-12m. GPR profile of line 40 (bottom of figure 5.3.25) also shows similar anomaly at 8-10m. We estimate these anomalies continue from the anomaly in Grid 1.

GRID 3: The GPR profile on line 20 in figure 5.3.26 shows an anomaly at 28-38m. The width of

Figure 5.3.22 Snapshot of the GPR survey (2008 - 2009 season)

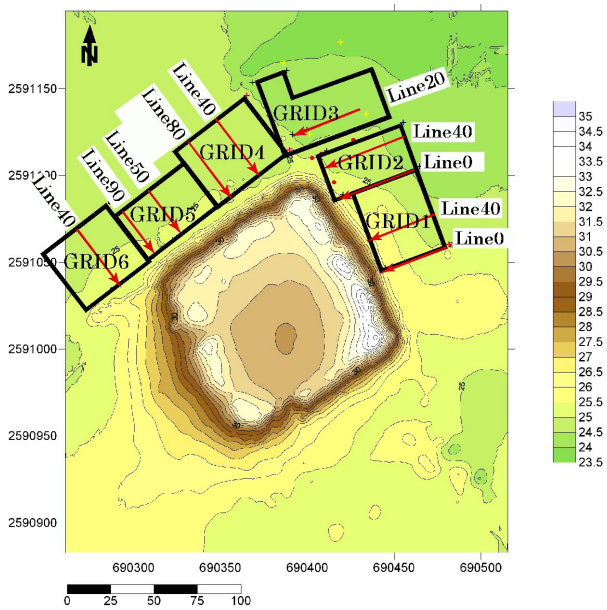

Figure 5.3.23 Areas of the GPR survey

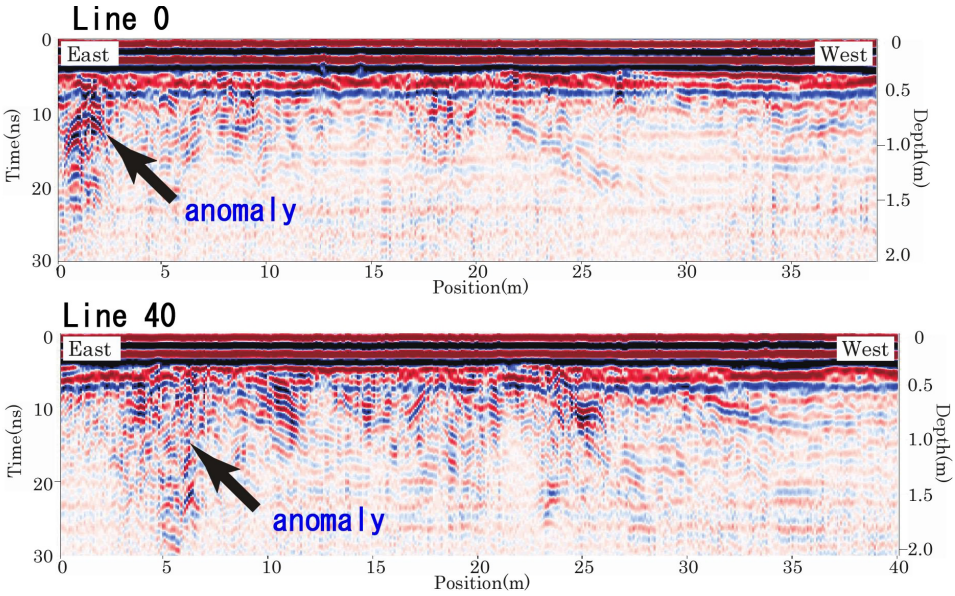

Figure 5.3.24 Representative GPR profile in Grid 1 (Line 0, Line 40)

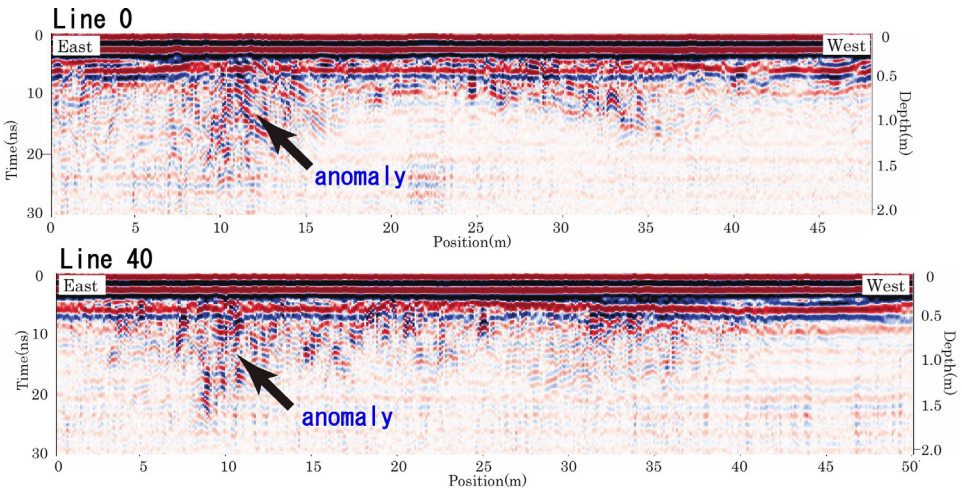

Figure 5.3.25 Representative GPR profile in Grid 2 (Line 0, Line 40)

anomaly is wider than the continuous anomalies in Grid 1 and Grid 2. The difference of width of anomalies may have been caused by obliquely crossing of the survey line and the belt like source of anomalies (stone piled wall), or by existence of big remain structure such as dwelling or building.

GRID 4: Figure 5.3.27 shows the GPR profile of line 40, which reaches to the edge of the Citadel mound. We could not identify the anomaly related to the stone objects like that detected in Grid 1-3. Around the area of 18-21m of the line, the GPR profile indicates the anomaly with ditch like structure, where the depth of bottom of anomaly is 0.8-1m. We estimate GPR anomaly indicates a natural stream or an artificial waterway.

We detected a ditch like structure around 25-30m of GPR profile at line 80 (bottom of figure 5.3.27). The depth of the deepest point of anomaly is 0.9m. There is only one ditch like structure at line 80 while two such structures exist at line 40. The width of the ditch like structure at line 80 is about 5m, which is 2 times wider than the width of anomaly at line 40. We estimate two ditches exist at the area of line 40, and they join around line 80.

GRID 5: The GPR profile of line 50 shows a structure of ditch (top of figure 5.3.28). A same ditch like structure is also detected at 33-39m of line 90 (bottom of figure 5.3.28).

Besides this anomaly, strong anomaly is identified at 28-30m of line 90, which has multiple reflections related to the stone objects like in Grid 1-3. We estimate a part of wall survived in this area.

GRID 6: GPR profile of line 40 shows the clear ditch like structure (Figure 5.3.29), which is similar to the structure detected in Grid 4 and 5. Another narrow anomaly at 41m extended to 2m depth may be the reflection caused by the survived metal waste.

2.2. Analysis by time-slice map

A time-slice map was created by synthetic analysis of GPR profiles of all survey lines at Grid 1-6. In Figure 5.3.30, time-slice map at the depth 1.08-1.35m is shown. The figure indicates that the GPR anomaly in Grid 1-3 extends straight (shown by red broken line in the figure) and turns at Grid 3.

The angle of the turn is about 82 degree. We estimate this turn structure is a corner of wall associated with the Citadel, because it seems to surround the Citadel mound and the shape of mound is rhombus prolonged north to south. In addition, the GPR survey in 2007 found that southern outer wall of the Citadel turns at about 86 degree. The anomaly indicating wall in Grid 3 shows partly hollow shape, which suggests the existence of a gate like facility.

The ditch like structure detected in Grid 1-4 extends from southwest to northeast, branches off to 2 ditches, and joins again in Grid 3 (partly shown by yellow broken line). It is difficult to distinguish whether the structure is a natural stream or an artificial waterway by the survey data. We suppose it is a natural stream, because it meanders and not goes side by side with the ruin of wall. As the level of surface descents from southwest to northeast in modern topography, we estimate that water flowed from southwest to northeast in those days.

There is a ‘ ㄱ ’ shaped anomaly at the boundary of Grid 5 and Grid 6. We estimate that it is a facility of the Citadel, because it exists next to the edge of Citadel as if it is attached to the mound. The ancient stream flows just like to penetrate the facility. We could not clarify which is older or newer of the stream and the facility, but if we could assume that they existed at same time,

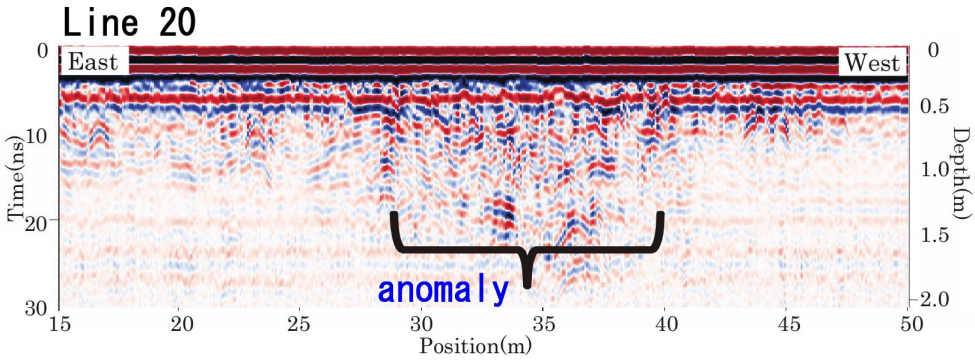

Figure 5.3.26 Representative GPR profile in Grid 3 (Line 20)

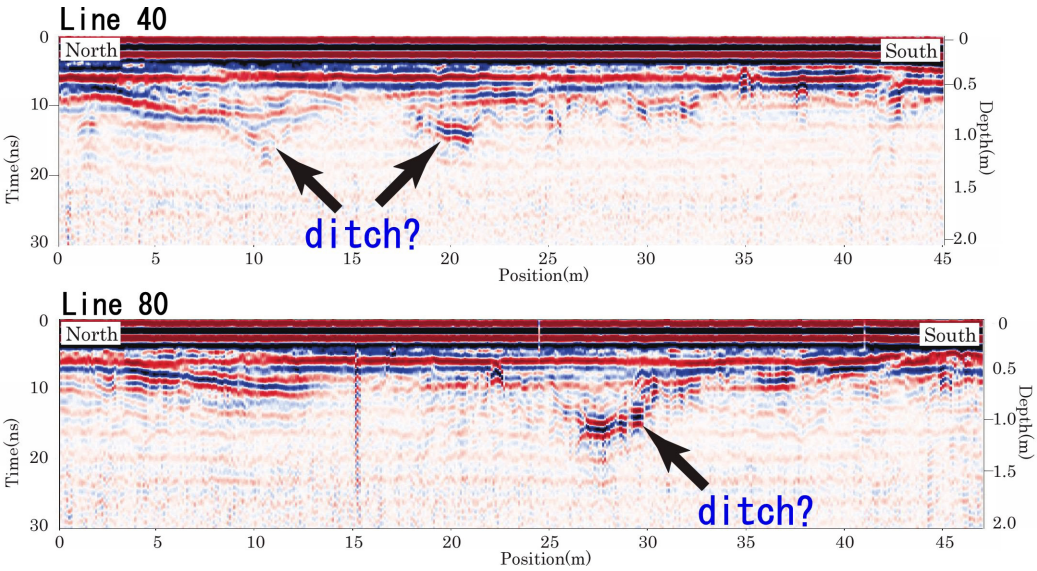

Figure 5.3.27 Representative GPR profile in Grid 4 (Line 40, Line 80)

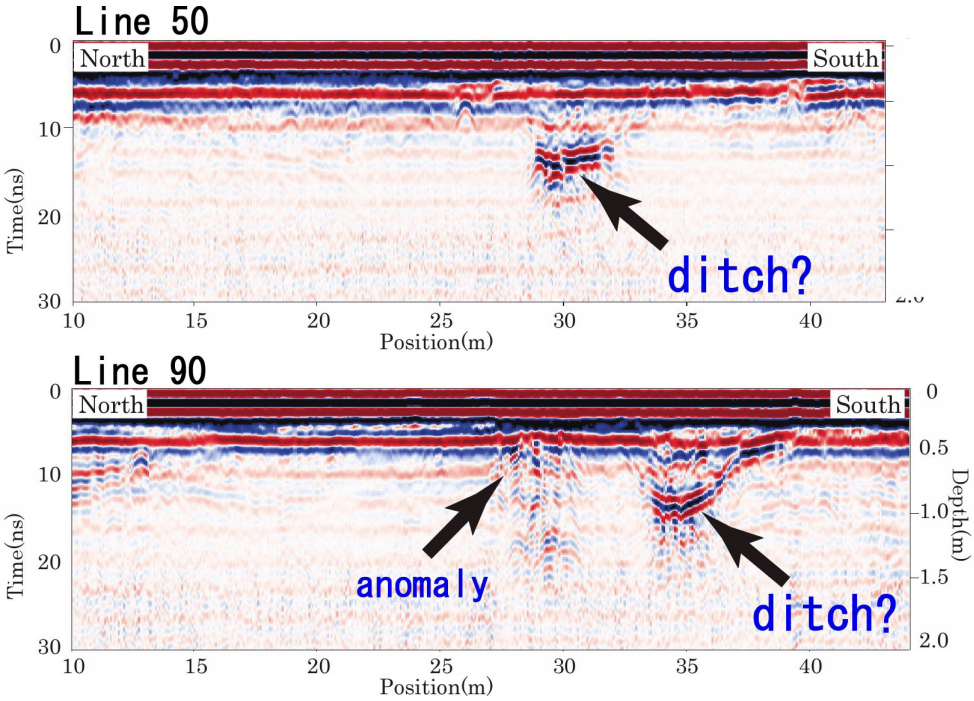

Figure 5.3.28 Representative GPR profile in Grid 5 (Line 40, Line 80)

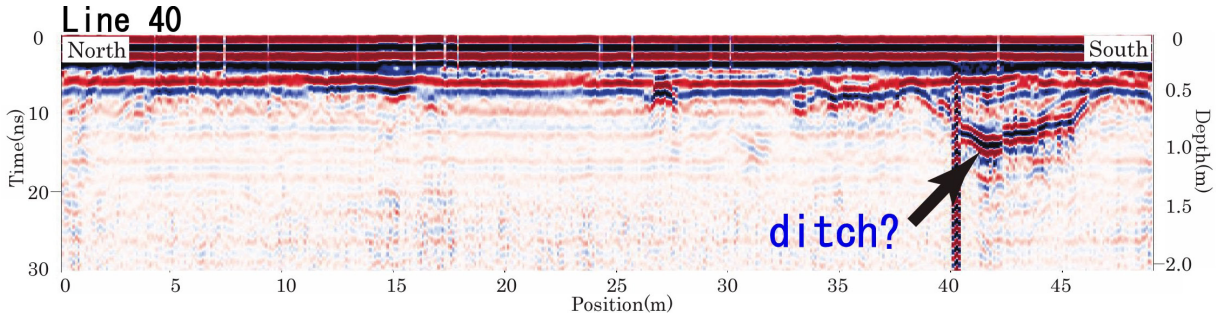

Figure 5.3.29 Representative GPR profile in Grid 6 (Line 40)

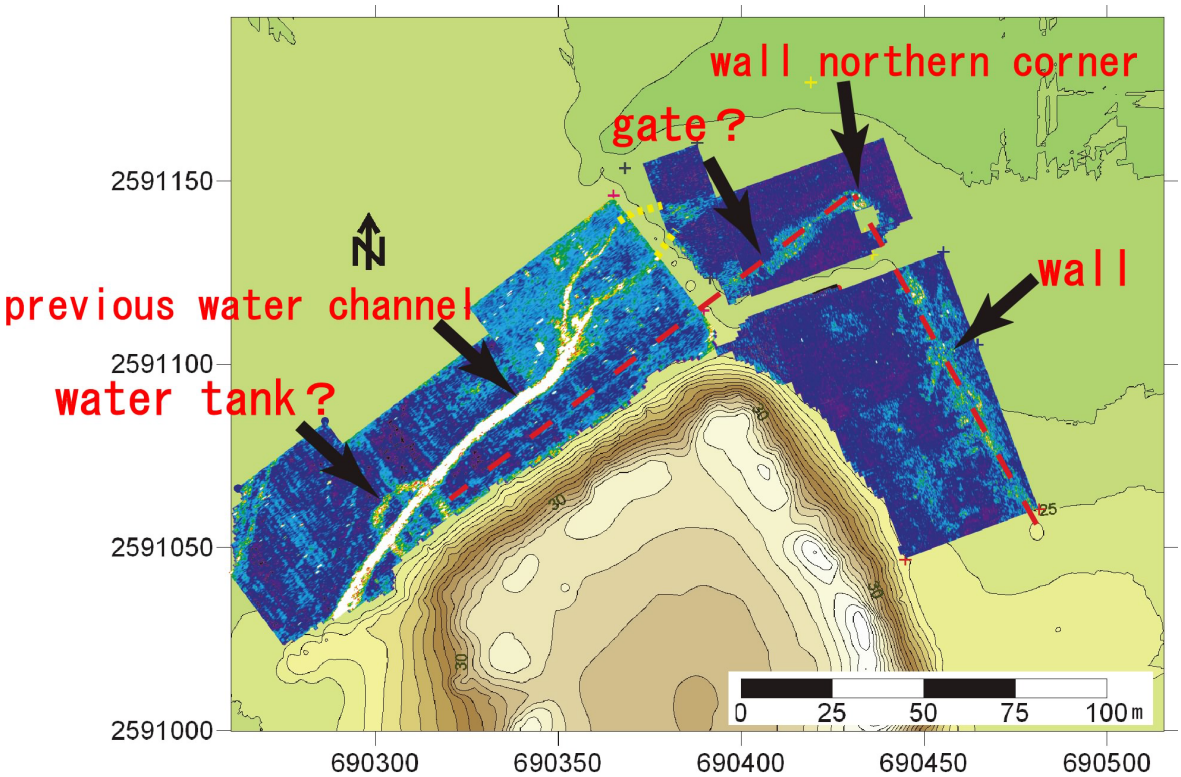

Figure 5.3.30 Results of the GPR survey (2008 - 2009 season)

the facility may have been a tank of water from the stream.

3. Conclusion

The GPR survey was carried out at adjoining area of northern edge of the Citadel mound in order to find attached facilities of the Citadel mound such as walls or dwellings.

GPR anomalies of stone piled walls were detected at northeastern and northwestern zone of the survey area and we could confirm the northern corner of the Citadel wall. There is a hollow like part of the wall at 30m south of the northern corner, which suggests a gate facility. We could also detect a stream of 4-5m width at the northwestern area of the Citadel mound. Further, ‘ コ ’ shaped anomaly which seems to draw a branch of the stream was found, and we could indicate the possibility of existence of a water tank there.

In this study, GPR survey detects the walls clearly. We think the fine survey results are obtained because of the existence of remain structures at comparatively shallow position (1.5m

depth from surface) and their well preservation.

Extent of remain structures related to Citadel mound is important factor to estimate the scale or power of the site. We think that we could clarify effectiveness of the method of reconstructing archaeological sites by combining geophysical survey with excavation.